Bacterial predator-prey coevolution selects on virulence-associated prey defences

Ramith R. Nair*[1,2], Marie Vasse*[1], Sébastien Wielgoss[1], Lei Sun[1], Yuen-Tsu N. Yu[1] and Gregory J. Velicer[1]

[1]Institute for Integrative Biology, ETH Zürich, Zürich, Switzerland
[2]Institute of Biology, Leiden University, Leiden, Netherlands
*co-first authors

Bacteria are estimated to constitute ~15% of Earth's biomass and contribute greatly to global resource turnover[1]. Predatory bacteria, pervasive throughout terrestrial and aquatic habitats[2,3], are likely to strongly influence such ecosystem processes and, given the importance of predators to macro-organismal communities[4–6], microbial community evolution as well[7–9]. Here we show that coevolution of a generalist bacterial predator (*Myxococcus xanthus*) with one species of bacterial prey (*Escherichia coli*) greatly alters patterns of fitness and genome evolution for both predators and prey and drives sympatric phenotypic diversification of prey. Following ~165 generations of evolution, coevolved prey outcompeted control-evolved prey in the presence of all predators (ancestral, control-evolved and coevolved) but not in their absence. Suggestive of Red Queen dynamics[10], coevolved predators were found to be more fit relative to their ancestor during consumption of coevolved prey than ancestral prey. Coevolved populations of both predators and prey exhibited greatly accelerated genome evolution relative to controls, including the rapid appearance of mutator genotypes in three coevolved communities. Both predators and prey underwent strong parallel evolution at selection hotspots specific to the coevolution treatment, with all 12 coevolved predator populations mutating at a locus not previously associated with *M. xanthus* predation. Reciprocally, predators drove strong parallel adaptations at two virulence-associated traits among prey- mucoidy[11] and the outer-membrane protease OmpT[12]. Mucoid variants appeared in 10/12 coevolved prey populations but in only one control. Further, 11/12 coevolved prey populations, but no controls, mutated at *ompT*, experimental deletion of which increased prey fitness in the presence of predators but not in their absence. These results with simple two-species communities suggest that generalist predatory bacteria are important determinants of how complex prey communities and their interaction networks evolve and diversify in natural habitats.

Antagonistic interactions, including parasitism and predation, play major roles in shaping the ecology and evolution of both macrobial[13] and microbial[14–17] species and communities. However, the potential of a major category of microbial predation, namely facultative generalist bacterial predators, to shape the evolution of prey species and community interaction networks has not been investigated. *M. xanthus*, a soil-dwelling delta-proteobacterium[18], kills and consumes a wide variety of microbial species, including *E. coli*, by largely unelucidated mechanisms[19], but can also subsist on complex growth substrates not derived directly from prey. To achieve a classic predator-prey interaction in which predators are trophically dependent on their prey, we provided glucose, which only the prey can utilise to fuel growth, as the sole carbon source in coevolution and both prey-only and predator-only control treatments (Fig. 1a, Extended data Table 1). Additionally, we used casitone-supplemented medium to allow predator survival in a second predator-only control treatment. After each 3.5-day growth cycle, 1% of evolving populations (controls) and communities (coevolution) were transferred to give ~6.6 generations of growth per day (although generation numbers may be somewhat increased for prey in coevolving populations due to killing by predators). As expected, the predator-only populations on glucose-minimal medium all rapidly went extinct (within five cycles), whereas all other populations of both predator and prey were maintained for 25 cycles, or ~165 generations. After evolution, adaptation was quantified with pairwise competitions between coevolved vs. control-evolved prey in the presence and absence of predators (ancestral, coevolved, and control-evolved) and between coevolved vs. ancestral predators in the presence and absence of prey (ancestral and coevolved). We modified an existing NGS-based method for measuring frequencies of genetically distinct bacterial competitors (FreqSeq[20]), to simultaneously estimate competitor frequencies from hundreds of competition experiments (Multiplex FreqSeq (Extended data Fig. 1, Tables 2 and 3). Control experiments showed Multiplex FreqSeq to estimate competitor frequencies with high accuracy (Extended data Fig. 2).

Coevolved prey populations were fitter compared to the control-evolved populations in all three predator contexts but not in the absence of predators, thereby indicating adaptive evolution of prey in response to general predation pressure (ANOVA, predator treatment: $F_{3,95} = 29.238$, $p = 1.77 \times 10^{-13}$, one-sample t-tests with Holm-Bonferroni correction; ancestral: $t_{11} = 3.78$, $p = 0.012$; coevolved: $t_{11} = 2.95$, $p = 0.027$; control-evolved: $t_{11} = 3.42$, $p = 0.017$; no predator: $t_{11} = -1.32$, $p = 0.21$; Fig. 1b, Extended data Fig. 3). Reciprocally, coevolved predators outcompeted their ancestors in all tested environments (including in the absence of prey; ANOVA, prey treatment: $F_{2,57} = 4.908$, $p = 0.0115$; one-sample t-tests with Holm-Bonferroni correction; coevolved prey: $t_8 = 6.38$, $p = 6.4 \times 10^{-4}$; ancestral prey: $t_{10} = 2.39$, $p = 0.038$; casitone: $t_{10} = 2.99$, $p = 0.027$, Fig. 1c, Extended data Fig. 4), but did so to a greater degree while consuming coevolved prey than with either ancestral prey or on casitone (Tukey multiple comparisons of means, coevolved vs ancestral $p = 0.047$, coevolved vs casitone $p = 0.011$). Collectively, these fitness patterns are suggestive of a "Red Queen" evolutionary scenario[10] involving generic predation-defence adaptations by prey and subsequent counter-adaptation by predators.

Coevolution was associated with striking patterns of both phenotypic and genotypic parallelism. Most coevolved prey populations contained readily detectable frequencies of mucoid variants during the experiment (cycle 18: 10/12 populations) while mucoidy was not detected in any control prey population except for a single colony in one population. These results are unlikely by chance (exact binomial test, $p < 0.001$), indicating that predation imposes positive selection for mucoidy, a known virulence trait in *E. coli*[11] that also reduces susceptibility to phage infection in other species of bacteria[21]. Consistent with this

inference, mucoid colonies were found to better resist predation than non-mucoid colonies (one-sided *t*-test: t_4 = -4.497, p = 0.005; Figs. 2a, b) and ancestral predators swarmed slower on mucoid than non-mucoid prey (one-sided *t*-test: t_4 = -2.4386, p = 0.036, Fig. 2c). The emergence of mucoid variants almost exclusively in coevolution populations shows that predators can drive prey diversification in simple bacterial communities with only one predator and one prey species[16], as seen in more complex ecosystems[22,23]. Moreover, experimental evolution of bacteria in the presence of lytic phages[21], macrophages[11] and antibiotics[24] has also caused the evolution of mucoidy, associating this phenotypic state with protection against an extremely divergent range of biological antagonists and weapons.

Antagonistic coevolution is expected to accelerate evolution at relevant loci[17] and does so among phage antagonists adapting to coevolving bacterial victims[25]. To investigate the impact of long-term bacterial predator-prey coevolution on the genomic evolution of both predatory antagonists and victims, we sequenced the genomes of three clones from each coevolved and control-evolved population of predators and prey. Even excluding mutator clones (which only appeared in coevolved populations), coevolution was found to accelerate genome evolution among prey, as coevolved clones accumulated ~2.7-fold more mutations on average than control-evolved prey clones (one-sided *t*-test: t_{11} = 5.07, p = 0.0002, Fig. 3). Coevolution also appears to have accelerated the genomic evolution of predators (one-sided *t*-test: t_{11} = 2.49, p = 0.015, Fig. 3). (However, due to the supplementation of predator-control media with casitone to allow predator survival, possible nutrient-source effects on predator genome evolution cannot be entirely excluded.)

Surprisingly, after less than 200 generations of evolution, 25% (3/12) of our coevolving communities evolved high frequencies of mutator clones in either the predator (ME4, 3/3 clones; and ME8, 2/3 clones, mutations in *mutS*) or the prey (ME1, 3/3 clones, mutation in *mutT*) populations. In comparison, among 12 *E. coli* B populations evolving as monocultures in a similar nutrient regime (but an unstructured environment), no populations had evolved mutators after 2000 generations (sample per population per time point n = 2) and only two had high-frequency mutators detected at 5000 generations (the next sampled generational time point)[26]. Mutators can hitchhike with beneficial mutations if the benefit of the latter offsets the load of deleterious mutations[27,28]. However, mutator mutations may themselves be transiently adaptive in novel or highly variable environments by generating adaptive mutations at a faster rate than non-mutators[29]. The extremely rapid fixation of mutators only among our coevolved populations suggests that predator-prey interactions may significantly increase the overall benefit/cost ratio of mutator phenotypes and further strengthens the accelerative effect of such interactions on the rate of genome evolution.

Concomitant with the phenotypic parallelism of mucoidy evolution among prey, coevolved populations of both predators and prey exhibited compelling patterns of parallel genotypic evolution, whereas control-evolved populations did not. Multiple loci among both prey and predator coevolved populations evolved in parallel (Figs. 4b,c; Extended data Tables 2, 3, 4 and 5), with extreme parallelism at *ompT* (Fig. 4a) among prey and an uncharacterized locus (*Mxan_RS27920*) among predators (Fig. 4b). *ompT* was mutated in 11 out of the 12 coevolved prey populations (19 clones out of 36), with no specific mutation shared by clones from distinct populations, but was not mutated in any of the six control-evolved populations (Fig. 4a). Many *ompT* mutations were multi-base deletions or generated premature stop codons, indicating predation-specific selection against *ompT* function.

ompT encodes an outer-membrane protease belonging to the omptin family that is a virulence factor among uropathogenic *E. coli* which targets antimicrobial peptides and protamines in the urinary tract[12,30,31]. As predicted from the mutational patterns among evolved clones, experimental deletion of *ompT* in the ancestral *E. coli* genetic background conferred a significant fitness advantage when competitions were performed with predation pressure from *M. xanthus* but not in the absence of the predator (ANOVA, predator treatment: $F_{1,16}$ = 8.42, p = 0.01, one-sample *t*-tests with Holm-Bonferroni correction; presence: t_{11} = 3.96, p 0.005 and absence: t_{11} = -1.006, p = 0.34; Fig. 4c, Extended data Fig. 5). Thus, long-term evolution with a bacterial predator simultaneously selects for and against distinct *E. coli* virulence factors (mucoidy and OmpT function, respectively).

Among the predators, the *Mxan_RS27920* locus was mutated or deleted in almost all clones from the 12 coevolved populations (34/36) but in none of the clones from casitone-evolved lineages, again with no specific mutations shared across populations. This gene (which we name *eatB)* encodes a predicted membrane protein belonging to the major facilitator super family, which contains proteins involved in transporting various solutes including sugars[32]. No association of *eatB* with predation was previously known, such that mechanistic investigation of how loss of this gene's function enhances fitness during consumption of *E. coli* should provide novel insights into the molecular mechanisms of *M. xanthus* predation.

Coevolution between just one bacterial predator and one prey in our simple system rapidly induced major evolutionary change at multiple bacterial traits known to be involved in interactions with additional and radically divergent antagonistic partners – animals and obligate phage parasites. Given this, generalist predatory bacteria in natural microbial communities can be expected to drive diversification and shape the evolution of complex interaction networks within those communities. Components of such networks include fitness relationships and modes of competition among diverse prey species, interactions both between those prey and other categories of predators (e.g. protists, nematodes, amoebae) and interactions among predators. With predatory bacteria being promoted as potential biocontrol agents in medicine[33–35] and agriculture[36,37], the induction of virulence-trait evolution found in our experiment indicates that such applied considerations should be informed by future evolution experiments with bacterial predators in systems of variable biological complexity.

Figure legends

Fig 1. Experimental coevolution system. a, Coevolved predator-prey communities (12) and control-evolved

predator or prey populations (six each) were propagated on minimal medium with glucose or casitone. Numbers below strain names are inoculum population sizes. b, Log-transformed relative fitness of coevolved prey over control-evolved prey when grown in the presence and in the absence of predators (n = 12). c, Log-transformed relative fitness of coevolved predator over ancestral predator when grown in the presence of prey and on casitone (n = 12). Grey dots are means of three replicates for each population. Black dots represent grand means across all populations within each treatment and error bars show 95% confidence intervals (*t*-distribution).

Fig 2. Phenotypic evolution of mucoidy among coevolved prey populations. a, Qualitative predation assay of *M. xanthus* (centre) on mucoid (left), non-mucoid (right) and ancestral (above) *E. coli* from seven coevolved populations. b, Swarming speed (relative to speed on ancestral prey) of the contemporary predator on lawns of mucoid and non-mucoid cells (n = 3). c, Percentage of contemporary mucoid and non-mucoid variants killed by the contemporary predator (n = 3). Grey dots are individual replicates. Black dots are means and error bars show 95% confidence intervals (*t*-distribution).

Fig 3. Predator-prey coevolution accelerated genome evolution. Significantly more mutations fixed or rose to high frequency among coevolved predator and prey populations than in control-evolved populations (n = 3 clones for each species for most individual populations, total n = 33 and n = 18 for coevolved and control-evolved prey populations, respectively; n = 31 and n = 8 for coevolved and casitone-evolved predator populations, respectively). Hypermutator clones (three clones from one prey population and five clones from two predator populations) were excluded, but would increase differences between genome-evolution rates of coevolved vs control-evolved populations yet more if included. Grey dots are means of three clones per populations and black dots and error bars are grand means and 95% confidence intervals (*t*-distribution) across all populations, respectively.

Fig 4. Parallel genetic evolution among coevolved populations. a, Parallel mutation of *ompT* among coevolved prey populations. b, Parallel mutation of *Mxan_RS27920* among coevolved predator populations. a, b, |, □, △, ▽ and dashed lines depict SNPs, duplications, small deletions (1-2bp), insertions and big deletions, respectively. Numbers in parentheses indicate the number of sampled clones (of three) in population sharing the adjacent mutation. c, Log-transformed relative fitness of an *ompT*-deletion mutant in competition with the ancestor in the presence and in the absence of the ancestral predator (n = 6 for both treatments). Grey dots are individual data points and black dots and error bars are respectively means and 95% confidence intervals (*t*-distribution).

Author contributions

RRN, GJV and MV designed the experiments. RRN, LS and MV performed the experiments. Y-TNY and SW developed methods. RRN, GJV. and MV analysed the data. RRN, GJV and MV wrote the manuscript. All authors read and approved the manuscript.

Competing interests

The authors declare no competing interests.

Acknowledgements

Thanks to Francesca Fiegna, Samay Pande, Fabienne Benz and Jessica Plucain for help with experiments. Thanks to Silvia Kobel, Niklaus Zemp and Aria Maya Minder Pfyl from the Genomic Diversity Centre at ETH Zurich for help during Multiplex FreqSeq development.

1. *Bar-On, Y. M., Phillips, R. & Milo, R. The biomass distribution on Earth.* Proc. Natl. Acad. Sci. *201711842 (2018). doi:10.1073/pnas.1711842115*
2. *Jurkevitch, E.* Predatory prokaryotes: biology, ecology and evolution. *(Springer Science & Business Media, 2006).*
3. *Pérez, J., Moraleda-Muñoz, A., Marcos Torres, F. J. & Muñoz-Dorado, J. Bacterial predation: 75 years and counting!* Environ. Microbiol. *n/a--n/a (2015). doi:10.1111/1462-2920.13171*
4. *Paine, R. T. Food Web Complexity and Species Diversity.* Am. Nat. ***100,*** *65–75 (1966).*
5. *Terborgh, J. & Estes, J. A.* Trophic Cascades: Predators, Prey, and the Changing Dynamics of Nature. Trophic Cascades: Predators, Prey, and the Changing Dynamics of Nature *(2010). doi:10.1016/j.ecolecon.2011.07.010*
6. *Estes, J., Crooks, K. & Holt, R. D. in* Encyclopedia of Biodiversity: Second Edition *(2013). doi:10.1016/B978-0-12-384719-5.00117-9*
7. *Corno, G. & Jürgens, K. Direct and indirect effects of protist predation on population size structure of a bacterial strain with high phenotypic plasticity.* Appl. Environ. Microbiol. ***72,*** *78–86 (2006).*
8. *Sherr, E. B. & Sherr, B. F. Significance of predation by protists in aquatic microbial food webs.* Antonie Van Leeuwenhoek ***81,*** *293–308 (2002).*
9. *Glücksman, E., Bell, T., Griffiths, R. I. & Bass, D. Closely related protist strains have different grazing impacts on natural bacterial communities.* Environ. Microbiol. *(2010). doi:10.1111/j.1462-2920.2010.02283.x*
10. *Van Valen, L. A new evolutionary law.* Evol. Theory ***1,*** *1–30 (1973).*
11. *Miskinyte, M.* et al. *The Genetic Basis of Escherichia coli Pathoadaptation to Macrophages.* PLoS Pathog ***9,*** *e1003802 (2013).*
12. *Brannon, J. R., Thomassin, J.-L., Desloges, I., Gruenheid, S. & Le Moual, H. Role of uropathogenic Escherichia coli OmpT in the resistance against human cathelicidin LL-37.* FEMS Microbiol. Lett. ***345,*** *64–71 (2013).*
13. *Estes, J. A., Crooks, K. & Holt, R. Predators, ecological role of.* Encycl. Biodivers. *(2001).*
14. *Müller, M. S., Scheu, S. & Jousset, A. Protozoa Drive the Dynamics of Culturable Biocontrol Bacterial Communities.* PLoS One ***8,*** *(2013).*
15. *Otto, S., Harms, H. & Wick, L. Y. Effects of predation and dispersal on bacterial abundance and contaminant biodegradation.* FEMS Microbiol. Ecol. ***93,*** *fiw241 (2017).*

16. *Gallet, R.* et al. *Predation and disturbance interact to shape prey species diversity.* Am. Nat. ***170,*** *143–154 (2007).*
17. *Brockhurst, M. A. & Koskella, B. Experimental coevolution of species interactions.* Trends Ecol. Evol. ***28,*** *367–375 (2013).*
18. *Reichenbach, H. The ecology of the myxobacteria.* Environmental Microbiology ***1,*** *15–21 (1999).*
19. *Muñoz-Dorado, J., Marcos-Torres, F. J., Garcia-Bravo, E., Moraleda-Muñoz, A. & Pérez, J. Myxobacteria: Moving, Killing, Feeding, and Surviving Together.* Front. Microbiol. ***7,*** *781 (2016).*
20. *Chubiz, L. M., Lee, M.-C., Delaney, N. F. & Marx, C. J. FREQ-Seq: A Rapid, Cost-Effective, Sequencing-Based Method to Determine Allele Frequencies Directly from Mixed Populations.* PLoS One ***7,*** *e47959 (2012).*
21. *Scanlan, P. D. & Buckling, A. Co-evolution with lytic phage selects for the mucoid phenotype of Pseudomonas fluorescens SBW25.* ISME J. *(2012).*
22. *Paine, R. T. A Note on Trophic Complexity and Community Stability.* Am. Nat. ***103,*** *91----{&} (1969).*
23. *Nosil, P. & Crespi, B. J. Experimental evidence that predation promotes divergence in adaptive radiation.* Proc. Natl. Acad. Sci. *(2006). doi:10.1073/pnas.0601575103*
24. *Piña, S. E. & Mattingly, S. J. The Role of Fluoroquinolones in the Promotion of Alginate Synthesis and Antibiotic Resistance in Pseudomonas aeruginosa.* Curr. Microbiol. ***35,*** *103–108 (1997).*
25. *Paterson, S.* et al. *Antagonistic coevolution accelerates molecular evolution.* Nature ***464,*** *275–278 (2010).*
26. *Tenaillon, O.* et al. *Tempo and mode of genome evolution in a 50,000 - generation experiment.* bioRXiv Prepr. http//dx.doi.org/10.1101/036806 ***536,*** *1–21 (2016).*
27. *Tenaillon, O., Toupance, B., Nagard, H. Le, Taddei, F. & Godelle, B. Mutators, population size, adaptive landscape and the adaptation of asexual populations of bacteria.* Genetics ***152,*** *485–493 (1999).*
28. *Scott Wylie, C., Ghim, C. M., Kessler, D. & Levine, H. The fixation probability of rare mutators in finite asexual populations.* Genetics ***181,*** *1595–1612 (2009).*
29. *Giraud, A.* et al. *Costs and benefits of high mutation rates: Adaptive evolution of bacteria in the mouse gut.* Science (80-.). ***291,*** *2606–2608 (2001).*
30. *Grodberg, J. & Dunn, J. J. Ompt Encodes the Escherichia-Coli Outer-Membrane Protease That Cleaves T7-Rna Polymerase During Purification.* J. Bacteriol. ***170,*** *1245–1253 (1988).*
31. *Hui, C. Y.* et al. *Escherichia coli outer membrane protease OmpT confers resistance to urinary cationic peptides.* Microbiol. Immunol. ***54,*** *452–459 (2010).*
32. *Reddy, V. S., Shlykov, M. A., Castillo, R., Sun, E. I. & Saier, M. H. The major facilitator superfamily (MFS) revisited.* FEBS J. *(2012). doi:10.1111/j.1742-4658.2012.08588.x*
33. *Willis, A. R.* et al. Injections of Predatory Bacteria Work Alongside Host Immune Cells to Treat Shigella Infection in Zebrafish Larvae. Current Biology ***26,*** *(2016).*
34. *Dwidar, M., Monnappa, A. K. & Mitchell, R. J. The dual probiotic and antibiotic nature of Bdellovibrio bacteriovorus.* BMB Rep. ***45,*** *71–78 (2012).*
35. *Shanks, R. M. Q.* et al. *An Eye to a Kill: Using Predatory Bacteria to Control Gram-Negative Pathogens Associated with Ocular Infections.* PLoS One ***8,*** *e66723 (2013).*
36. *Scherff, R. H. Control of bacterial blight of soybean by Bdellovibrio bacteriovorus.* Phytopathology *(1973).*
37. *Rashidan, K. K. & Bird, D. F. Role of predatory bacteria in the termination of a cyanobacterial bloom.* Microb. Ecol. ***41,*** *97–105 (2001).*

Materials and methods

Predator-prey experimental coevolution

Ancestral strains

Three sub-clones each of streptomycin sensitive and resistant (*rpsL*, K43R; donated by Dr. Balazs Bogos, ETH Zurich) *Escherichia coli* MG1655 were isolated by streaking frozen glycerol stocks onto LB[38] agar plates. These sub-clones were grown to stationary phase in LB medium (37 °C, 200 rpm for 8-10 hours) and used to initiate 12 replicate populations coevolving with *M. xanthus* (two from each sub-clone) and six replicate prey-only populations (one from each sub-clone).

Myxococcus xanthus strain DK3470 was used as the predator[39]. This strain has a mutation (previously inferred to be in or near *the dsp*[39]*/dif*[40] gene region) that greatly reduces extracellular matrix production[39] and thus allows cultures to be readily dispersed in liquid buffer even after growth on an agar surface. Sub-clones of rifampicin sensitive and resistant (spontaneous mutants) variants of DK3470 were isolated from colonies grown in CTT soft 0.5% agar (10 g/l casitone, 10 mM Tris pH 8.0, 8 mM $MgSO_4$, 1 mM KPO_4) at 32 °C after dilution plating from mid-exponential phase 8 ml liquid CTT cultures (32 °C, 300 rpm). Three sub-clones of each genotype were isolated, stored frozen and used to initiate predator-only control populations - six on minimum medium (M9) supplemented with glucose and six on M9-casitone medium (details below), and 12 populations coevolving with *E. coli* (one, one and two populations founded from each DK3470 sub-clone, respectively; Extended data Table 1). Three of the casitone predator-only populations were discarded due to contamination during evolution. The remaining three were analyzed.

Predator-prey coevolution arena

The experimental coevolution protocol is summarized in Fig. 1a. Coevolution was performed in 50 mL conical flasks containing 8 mL solid media (1x M9 salts, 2 mM $MgSO_4$, 0.1 mM $CaCl_2$, 0.2% glucose, 1.5% agar; hereafter called prey-growth agar). We adjusted the densities of *E. coli* and *M. xanthus* populations by resuspending, respectively, ~10^5 *E. coli* cells and ~10^9 *M. xanthus* per 50 µL in TPM buffer (10 mM Tris pH 8.0, 8 mM $MgSO_4$, 1 mM KPO_4). To initiate the coevolution populations, we mixed 50 µL each of adjusted prey and predator cultures and spread the total volume on prey-growth agar with 7-9 sterile glass beads. For prey-only controls, 50 µL of adjusted *E. coli* culture was mixed with 50 µL of TPM buffer. We set two types of predator-only controls by spreading the adjusted *M. xanthus* cultures with 50 µL of TPM buffer onto both prey-growth agar and onto medium identical to prey-growth agar except that glucose was replaced with 0.5% casitone (a pancreatic digest of casein that *M. xanthus* can utilize as a carbon-substrate for growth). All flasks dried in a laminar-flow hood for about 30 minutes before incubation at 32°C, 90% rH for ~84 hours.

After ~84 hours of incubation, the predator-prey communities were harvested by adding 5 mL TPM buffer and shaking for ~15 minutes at 300 rpm at 32°C until the cultures were well suspended and dispersed. 1% (50 µL) of the resuspended cultures was then mixed with 50 µL of TPM buffer and spread onto fresh prey-growth agar as described above to initiate a new cycle. The evolution experiment ran for 25 such cycles, with frozen stocks made of evolving populations and communities after every second cycle starting at cycle 0 (in 20% glycerol, stored at -80°C) and after the terminal cycle. The presence of predators and prey was checked every second cycle by dilution-plating on LB agar (for prey) and on CTT soft-agar containing 10 µg/mL gentamicin (for predators). *M. xanthus* DK3470 cannot grow on LB medium (due to the salt concentration) and *E. coli* is sensitive to gentamicin while *M. xanthus* is naturally resistant. The presence of both predator and prey populations at consistent densities through the experiments suggests that both predator and prey populations gave ~6.6 generations between cycles.

Post-evolution fitness assays

To assess reciprocal adaptation, we performed fitness assays by competing coevolved populations vs. control-evolved or ancestral populations (Figs. 1b and 1c, Extended data Figs. 3 and 4). *E. coli* and *M. xanthus* were isolated from coevolved populations through inoculation in LB and gentamicin-CTT as described above. All competition experiments were performed in three temporally separate replicates with whole-population samples of evolved prey and/or predator populations.

Prey competitions

Prey populations were grown in LB as described above. Cultures were adjusted to an optical density (OD_{600}) of ~1.0 (~10^8 cells/ml) and 500 µL of each coevolved prey population were mixed with 500 µL of one control-evolved population with the opposite streptomycin-resistance marker type. We diluted these mixes (1:100) and inoculated 50 µL together with 50 µL of either a predator culture (~5 x 10^9 cells in TPM) or TPM buffer and spread onto prey-growth agar as described above. Predator cultures (ancestral, control-evolved and coevolved) were incubated in liquid gentamicin-CTT (10 µg/mL, 32°C, 300 rpm) for ~60 hours, upon which they were diluted and grown for further 8 – 10 hours to obtain mid-exponential cultures (OD_{600} ~0.5 – 0.8), which were subsequently centrifuged and resuspended in TPM buffer after supernatant removal. Each competition of co-evolved vs. control-evolved prey was subjected to four predator treatments: (i) the sympatrically coevolved predator, (ii) a control predator population that evolved on casitone medium in the absence of prey, (iii) the ancestral predator, (iv) no predator. In addition, all 12 coevolved and all six control-evolved prey populations were competed against the ancestral prey (of the opposite marker state) in the presence of all three predator categories (Extended data Fig. 6). Competition flasks were incubated at 32°C, 90% rH for 84 hours and harvested using the aforementioned protocol. We centrifuged 2 mL of resuspended culture (12000 rpm, 5 mins) and stored the pellets at -20°C until lysate preparation. Pellets of the initial mixes were obtained and stored similarly.

Predator competitions

Because all predator-only populations inoculated in prey-growth agar went extinct and predators growing on casitone are not perfect controls for the coevolution treatment due to the substitution of carbon source, we competed coevolved predators with their ancestors to test for predator adaptation. In preliminary experiments, we found that predator populations initially decline substantially when transferred directly from CTT to prey-growth agar prior to subsequently growing on prey. Thus,

for competition experiments we first pre-conditioned predator populations separately for three 84-hour cycles on prey-growth agar in the presence of the prey used in the subsequent assay. After three cycles of acclimatisation, populations were harvested as described before and stored at -20°C for lysate preparation. We prepared competition mixes and inoculated 100 µL of each mix onto prey-growth agar. The competition experiment was conducted for another three cycles. The remainder of the initial (T_0) mixes was spun down and stored at -20°C for lysate preparation.

Estimating relative fitness using Multiplex FreqSeq

Lysates of both prey and predator competition assays were prepared using the Triton X-100 protocol described by Goldenberger *et al*[41]. The resulting supernatant was used for the Multiplex FreqSeq library preparation described below.

We modified the FreqSeq method[20] to introduce a second barcode which allows multiplexing. Multiplex FreqSeq is described in Extended data Fig. 1 and the validation method in Extended data Fig. 2. A combination of two barcodes was used to label all populations involved in the competitions: each pair of right-side and left-side barcodes therefore identified one replicate of a given competition treatment. The primers and PCR conditions for Multiplex FreqSeq are detailed in Extended data Tables 6 and 7. DNA libraries were normalised, pooled and purified (Ampure XP beads) and their final sizes and concentrations were confirmed using an Agilent Bioanalyser. The pooled library was then diluted to 4 nM in water and run on a MiSeq machine at the Genomic Diversity Centre at ETH Zurich after mixing with 30% standard PhiX library. We ran one and nine MiSeq sequencing for prey and predator competitions, respectively. Data from MiSeq were checked for quality using FastQC and Illumina adapters were removed using Trimmomatic v0.33[42] with the parameters: ILLUMINACLIP:adapter.fa:2:30:10, to leave the six nucleotide barcode at the 3' end. The reads were demultiplexed using the barcode splitter algorithm in the FASTX-Toolkit (http://hannonlab.cshl.edu/fastx_toolkit/). Demultiplexed reads were stored as separate fastq files for each right-side barcode and analysed using the Freq-Out program[20] to obtain frequencies of each competitor from pre- and post-competition mixes. A bash script for running each step of data analysis in a single script is provided in the Extended data. Frequency estimates from unexpected barcodes, with less than 10000 reads or beyond the range tested in the validation assay (0.05 - 0.95, Extended data Fig. 2) were discarded.

We calculated the relative fitness of the coevolved prey or predators using the formula of Ross-Gillespie *et al.*[43]

$$v = \frac{x2(1-x1)}{x1(1-x2)}$$

where $x1$ and $x2$ are initial and final frequencies of the coevolved cells, respectively.

Prey phenotypic evolution

Screen for mucoid variants

Aliquots of frozen stocks of coevolved and control-evolved prey populations from cycle 18 were thawed in 100 µL TPM buffer, dilution plated onto LB agar and screened for the presence of mucoid colonies after overnight incubation at 32°C, 90% rH.

Predation resistance assays

We conducted a series of experiments to assess whether mucoidy could confer resistance against the predators. We first qualitatively assessed the ability of an expanding predator swarm to penetrate and lyse adjacent colonies of coevolved mucoid, coevolved non-mucoid and ancestral (non-mucoid) prey (Fig. 2a). For seven coevolved communities, one evolved mucoid clone, one evolved non-mucoid clone and ancestral *E. coli* were grown in LB to OD_{600} ~1.0 and 10 µL were spotted on both prey-growth and on CTT agar at a 1 cm-distance from a 10 µL *M. xanthus* spot (5 x 10^9 cells/mL). The plates were incubated (32°C, 90% rH) and predator-prey colony interface phenotypes were observed every 24 hours. The image shown in Fig. 2a was taken after five days of incubation.

We further quantitatively assayed prey resistance to *M. xanthus*, using one isolated mucoid clone and one non-mucoid clone from population ME4 (cycle 18). We measured the swarming rate of the predator on the different prey types (coevolved mucoid, coevolved non-mucoid and ancestral, Fig. 2b). We spotted ancestral *M. xanthus* (10 µL at 5 x 10^9 cells/mL) on top of a 48-hour old *E. coli* lawn on prey-growth agar and allowed it to swarm for 7 days (32°C, 90% rH). Swarm edges were outlined after one day and seven days, and migration distances were measured on opposite sides of at least three separate transects (thus at least six measurements per plate).

To compare the killing efficiency of ancestral *M. xanthus* for the different prey types, we inoculated mucoid and non-mucoid clones in the presence and absence of ancestral predators as in the coevolution experiment (Fig. 2c). After 84 hours, we assessed the percentage of killed prey as the reduction in population size due to the presence of the predators. *E. coli* population sizes were estimated by dilution-plating on LB agar. For all assays, we performed 3 biological replicates with 2 technical replicates each.

Genomic evolution

Whole genome sequencing

At transfer cycle 25 of the evolution experiment, three independent predator and/or prey clones each were randomly picked from either LB agar (prey), or gentamycin-CTT agar (predators) for all control-evolved and coevolved populations. Isolated predator and prey clones were grown in 8 mL CTT and LB, respectively. Grown cultures were centrifuged at 5000 rpm for 15 minutes and pellets stored at -80°C until DNA was extracted. Whole genomic DNA was isolated with Qiagen's Genomic DNA extraction buffer kit and 20/G Genomic-tips by following the manufacturer's recommendations, the quality of which was checked with Qubit. The whole genomes of predator and prey populations were sequenced on different Illumina® HiSeq® 2500 sequencing machines in paired-end mode; prey populations were processed by Fasteris (Geneva, Switzerland) producing reads of 125 bp while predator genomes were handled by the D-BSSE Quantitative Genomics Facility of ETH Zurich (Basel, Switzerland) also with a read length of 125 bp.

After initial quality assessment using FastQC (http://www.bioinformatics.babraham.ac.uk/projects/fastqc/), we removed Illumina-specific adapters/primers as well as low quality bases from all read sequence data using Trimmomatic v0.33[42]; with the following basic parameters:
ILLUMINACLIP:Nextera+TruSeq3-PE2.fa:2:25:10
CROP:124 HEADCROP:5 LEADING:30 TRAILING:28

SLIDINGWINDOW:4:28 MINLEN:77. The trimmed reads from *E. coli* prey populations were subsequently mapped to the *E. coli* str. K-12 substr. MG1655 reference genome[44] using breseq 0.27.0[45]. The latter step also involved error correction and variant calling (based on samtools v 1.3.1[46]; see Extended data Tables 2 and 3 for a summary mutation summary for all prey populations). In addition, the trimmed reads for control-evolved, co-evolved and ancestral predator clones were mapped to a manually revised reference genome of *M. xanthus* str. DK1622 using breseq 0.27.0 as described above (see Extended data Tables 4 and 5). That novel genomic reference contains all mutations present in the experiment's founding clone, an isolate of the ancestral strain DK3470, relative to its parent strain, *M. xanthus* str. DK1622 (**refseq**: NC_008095). Our ancestral clone of DK3470 and all evolved descendants sequenced for this study (details below) were found to carry a single base-pair deletion in the intergenic region between *Mxan_RS32420* (*difA*) and *Mxan_RS32425* (*thiL*) (43 bp downstream of *difA* and 1386 bp upstream of *thiL*). We infer this mutation to be the causal mutation responsible for the non-cohesive growth of DK3470 and that originally identified by linkage to a transposon Tn5 insertion[39]. The co-linked Tn5 transposon was found to have inserted into the coding sequence of gene *Mxan_RS32435*[39]. The Tn5 transposon tag carries three resistance genes against the antibiotics neomycin/kanamycin, bleomycin and streptomycin. Technically, mutations were screened for by mapping trimmed reads of the DK3470 genome against reference genome *M. xanthus* str. DK1622 using breseq 0.27.0; the sequence and precise location of the Tn5 transposon was inferred from a whole genome assembly with the same trimmed Illumina® reads using SPAdes v. 3.11.1[47] with parameters spades.py -k 21,33,55,77 --careful.

ΔompT prey mutant construction and fitness

ΔompT mutant construction

ΔompT-mutants were constructed by replacing the coding sequence of the *ompT* gene with a kanamycin resistance marker via recombineering[48]. The streptomycin-sensitive and resistant ancestral *E. coli* strains were transformed with the recombineering plasmid pSIM6 and maintained at 30°C degrees with 100 mg/L ampicillin in the media. The kanamycin marker was amplified from the KEIO strain JW0554[49] with PCR primers *ompT*-F (GTTACATTGAAATGGCTAGTTATTCCCC) and *ompT*-R (CAGTGGAGCAATATGTAATTGACTC). The purified PCR product was then used to replace *ompT* in both *E. coli* strains with pSIM6 (for a detailed recombineering protocol, see[48]). Positive clones were confirmed by growth on media with 100 mg/L kanamycin and sequencing with the aforementioned primers. To ensure a clean genetic background, P1 transduction was performed using the constructed *ΔompT* strains as donor and the ancestral strains as recipient[50]. Positive P1-transductants were confirmed by kanamycin resistance, colony-PCR and sequencing. All the subsequent fitness assays were performed using the P1-transduced strains.

Relative fitness of ΔompT prey

We estimated the relative fitness of *ΔompT* prey in competition with ancestral *E. coli* under the conditions of the post-evolution fitness assays (Fig. 4c, Extended data Fig. 5). Wildtype strains competed against Δ*ompT* mutant of opposite marker for one cycle (84 hours) in the prey-growth medium in the presence and in the absence of ancestral predators. Initial and final frequencies of each strain were determined by dilution-plating onto LB agar (plain and supplemented with 100 µg/mL streptomycin). To control for any marker effect, we also conducted competitions with clones of the opposite marker type but same *ompT* genotype. Relative fitness was calculated as described above. At least six independent replicates for each competition were performed.

Statistical analysis

We analyzed relative fitness of prey and predators with analysis of variance (ANOVA type II). For coevolved prey, we used predator treatment (coevolved, control-evolved, ancestral or no predator), population ID (ME1 to ME12) and competitor ID (control-evolved *E. coli* E^c1 to E^c6) as factors. For coevolved predators, we used prey treatment (coevolved, ancestral or casitone), population ID (ME1 to ME12) and competitor ID (rifampicin-resistant or sensitive ancestor) as factors. Post-hoc tests were Tukey-tests for multiple comparisons and one-sample *t*-tests with Holm-Bonferroni corrections. For the *t*-tests, data were the mean of three replicate competitions per coevolved population so that the unit of replication was each coevolved population (n = 12). For the prey *ompT* mutant, explanatory factors were predator treatment (presence or absence), time of the experiment (day 1 or day 2) and the resistance phenotype of the mutant (streptomycin resistant or sensitive). We log-transformed all relative fitness data to meet the assumption of normality.

The statistical analysis was performed using R studio (version 1.0.136)[51] and the packages car[52] and ggplot[53].

Data availability

Data are available on Dryad and GenBank.

38. *LB (Luria-Bertani) liquid medium.* Cold Spring Harb. Protoc. ***2006,*** *pdb.rec8141 (2006).*
39. *Shimkets, L. J. Role of cell cohesion in Myxococcus xanthus fruiting body formation.* J. Bacteriol. ***166,*** *842–848 (1986).*
40. *Yang, Z.* et al. *Myxococcus xanthus dif genes are required for biogenesis of cell surface fibrils essential for social gliding motility.* J. Bacteriol. *(2000). doi:10.1128/JB.182.20.5793-5798.2000*
41. *Goldenberger, D., Perschil, I., Ritzler, M. & Altwegg, M. A simple 'universal' DNA extraction procedure using SDS and proteinase K is compatible with direct PCR amplification.* PCR Methods Appl. ***4,*** *368–370 (1995).*
42. *Bolger, A. M., Lohse, M. & Usadel, B. Trimmomatic: a flexible trimmer for Illumina sequence data.* Bioinformatics ***30,*** *btu170---- 2120 (2014).*
43. *Ross-Gillespie, A., Gardner, A., West, S. A. & Griffin, A. S. Frequency dependence and cooperation: theory and a test with bacteria.* Am. Nat. ***170,*** *331–342 (2007).*
44. *Blattner, F. R.* et al. *The Complete Genome Sequence of Escherichia coli K-12.* Science ***277,*** *1453–1462 (1997).*
45. *Barrick, J. E.* et al. *Identifying structural variation in haploid microbial genomes from short-read resequencing data using breseq.* BMC Genomics ***15,*** *1 (2014).*
46. *Li, H. A statistical framework for SNP calling,*

mutation discovery, association mapping and population genetical parameter estimation from sequencing data. Bioinformatics *(2011). doi:10.1093/bioinformatics/btr509*

47. *Nurk, S.* et al. *Assembling genomes and mini-metagenomes from highly chimeric reads. in* Lecture Notes in Computer Science (including subseries Lecture Notes in Artificial Intelligence and Lecture Notes in Bioinformatics) *(2013). doi:10.1007/978-3-642-37195-0_13*
48. *Sharan, S. K., Thomason, L. C., Kuznetsov, S. G. & Court, D. L. Recombineering: A homologous recombination-based method of genetic engineering.* Nat. Protoc. *(2009). doi:10.1038/nprot.2008.227*
49. *Baba, T.* et al. *Construction of Escherichia coli K-12 in-frame, single-gene knockout mutants: the Keio collection.* Mol. Syst. Biol. ***2,*** *2006.0008 (2006).*
50. *Thomason, L. C., Costantino, N. & Court, D. L. E. coli genome manipulation by P1 transduction.* Curr. Protoc. Mol. Biol. ***Chapter 1,*** *Unit 1.17----1.17.8 (2007).*
51. *RStudio Team. RStudio: Integrated Development for R.* [Online] RStudio, Inc., Boston, MA URL http//www. rstudio. com *(2016). doi:10.1007/978-81-322-2340-5*
52. *Fox, J.* et al. *An R Companion to Applied Regression, Second Edition.* R topics documented *(2014).*
53. *Wickham, H., Winston, C. & RStudio. ggplot2: Create Elegant Data Visualisations Using the Grammar of Graphics.* CRAN *(2016). doi:10.1093/bioinformatics/btr406*

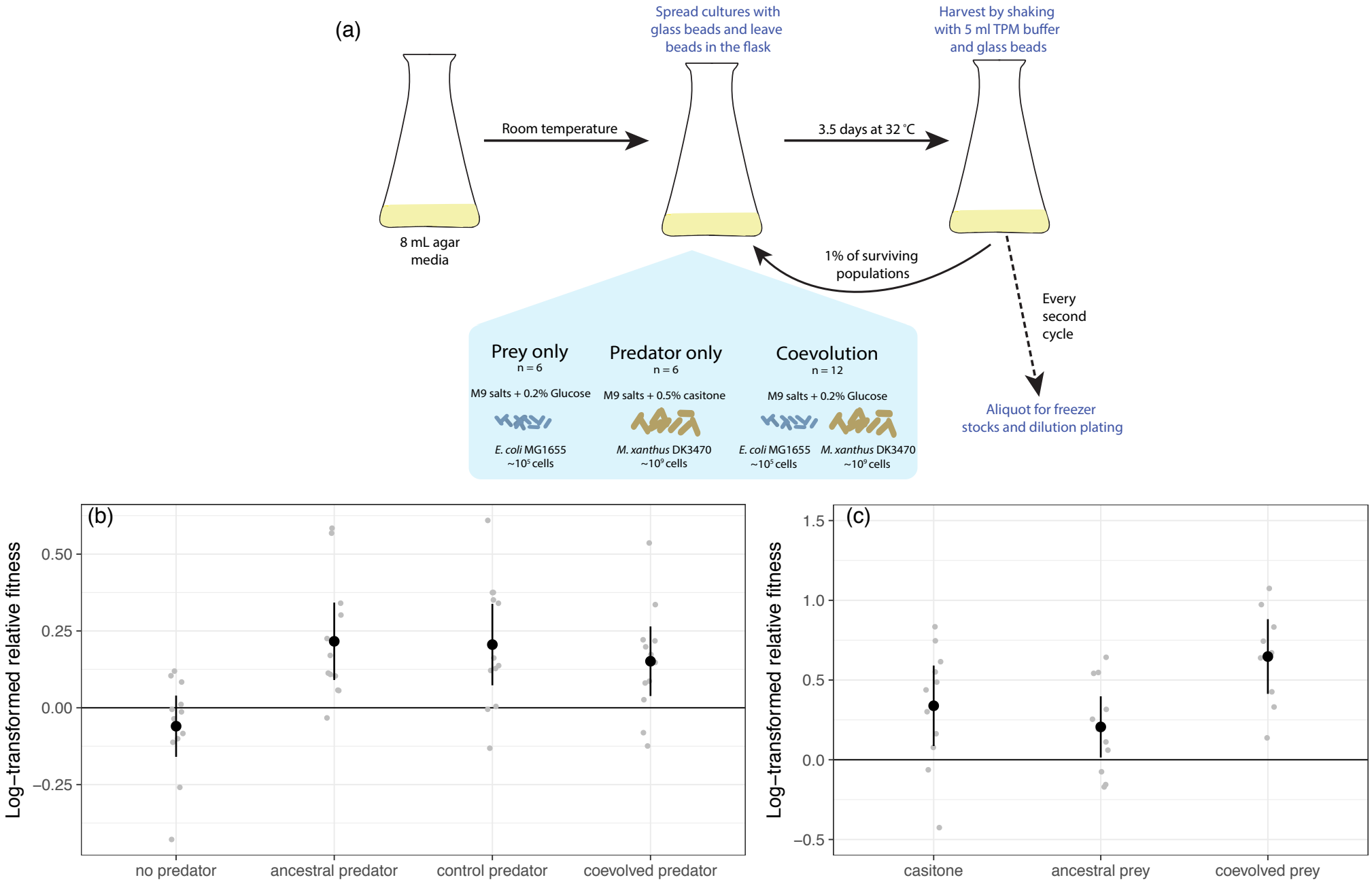
(a)
Spread cultures with glass beads and leave beads in the flask
Harvest by shaking with 5 ml TPM buffer and glass beads
Room temperature
3.5 days at 32 ˚C
8 mL agar media
1% of surviving populations
Every second cycle
Aliquot for freezer stocks and dilution plating
Prey only
n = 6
M9 salts + 0.2% Glucose
E. coli MG1655
~10⁵ cells
Predator only
n = 6
M9 salts + 0.5% casitone
M. xanthus DK3470
~10⁹ cells
Coevolution
n = 12
M9 salts + 0.2% Glucose
E. coli MG1655
~10⁵ cells
M. xanthus DK3470
~10⁹ cells
(b)
Log−transformed relative fitness
0.50
0.25
0.00
−0.25
no predator
ancestral predator
control predator
coevolved predator
(c)
Log−transformed relative fitness
1.5
1.0
0.5
0.0
−0.5
casitone
ancestral prey
coevolved prey

Fig. 1

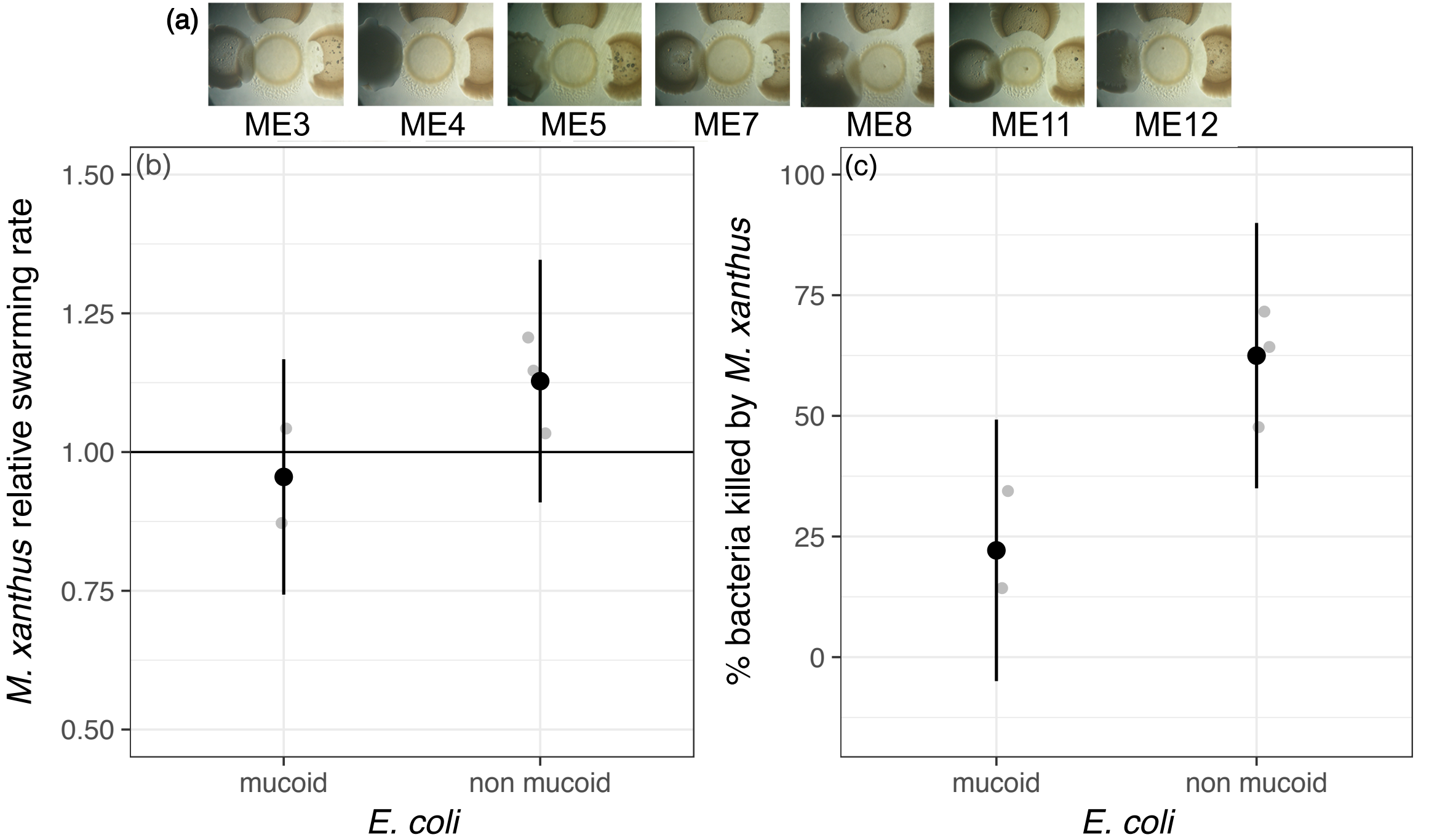
(a)
ME3
ME4
ME5
ME7
ME8
ME11
ME12
(b)
M. xanthus relative swarming rate
1.50
1.25
1.00
0.75
0.50
mucoid
non mucoid
E. coli
(c)
% bacteria killed by M. xanthus
100
75
50
25
0
mucoid
non mucoid
E. coli

Fig. 2

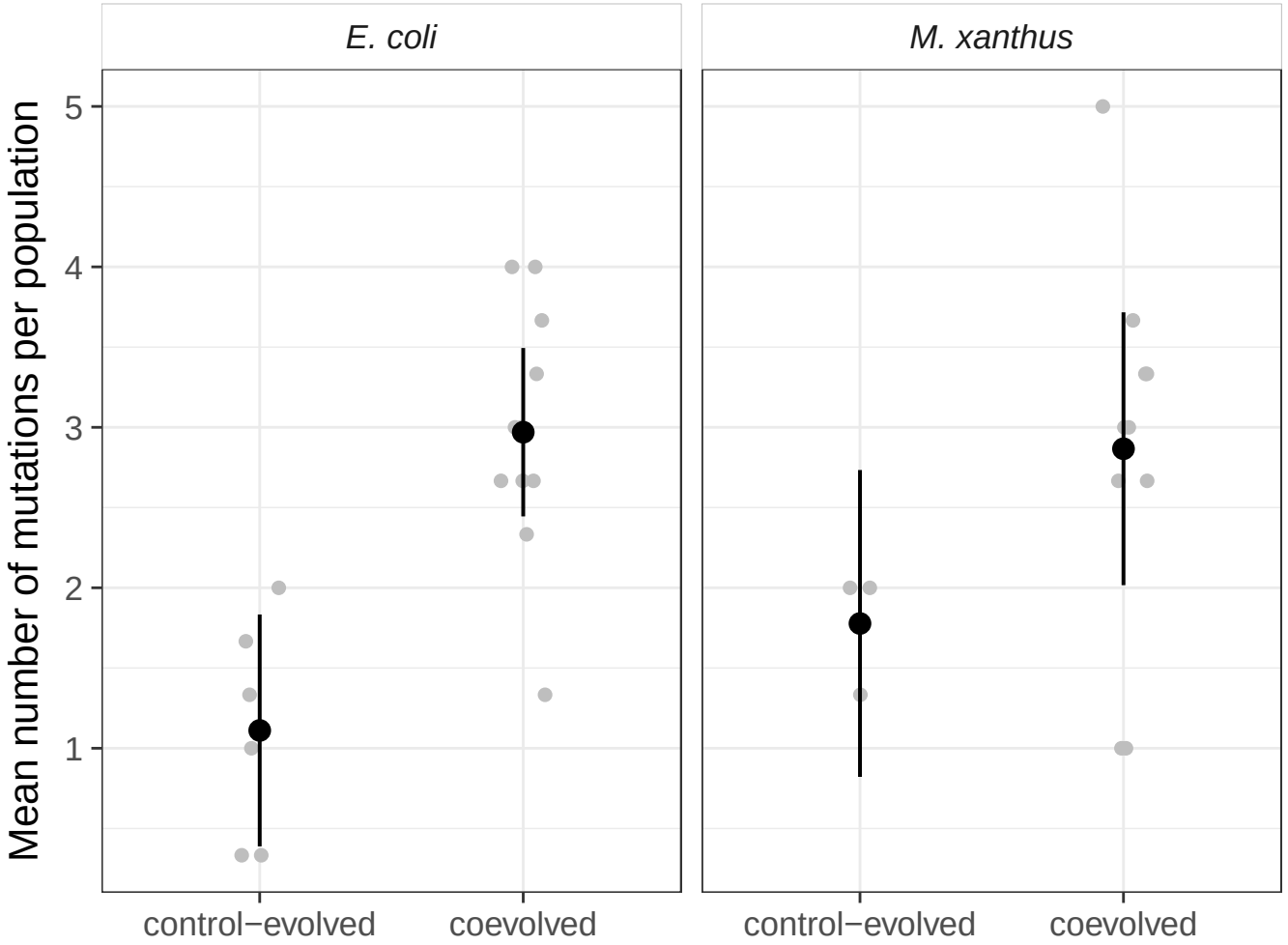
E. coli
M. xanthus
Mean number of mutations per population
5
4
3
2
1
control−evolved
coevolved
control−evolved
coevolved

Fig. 3

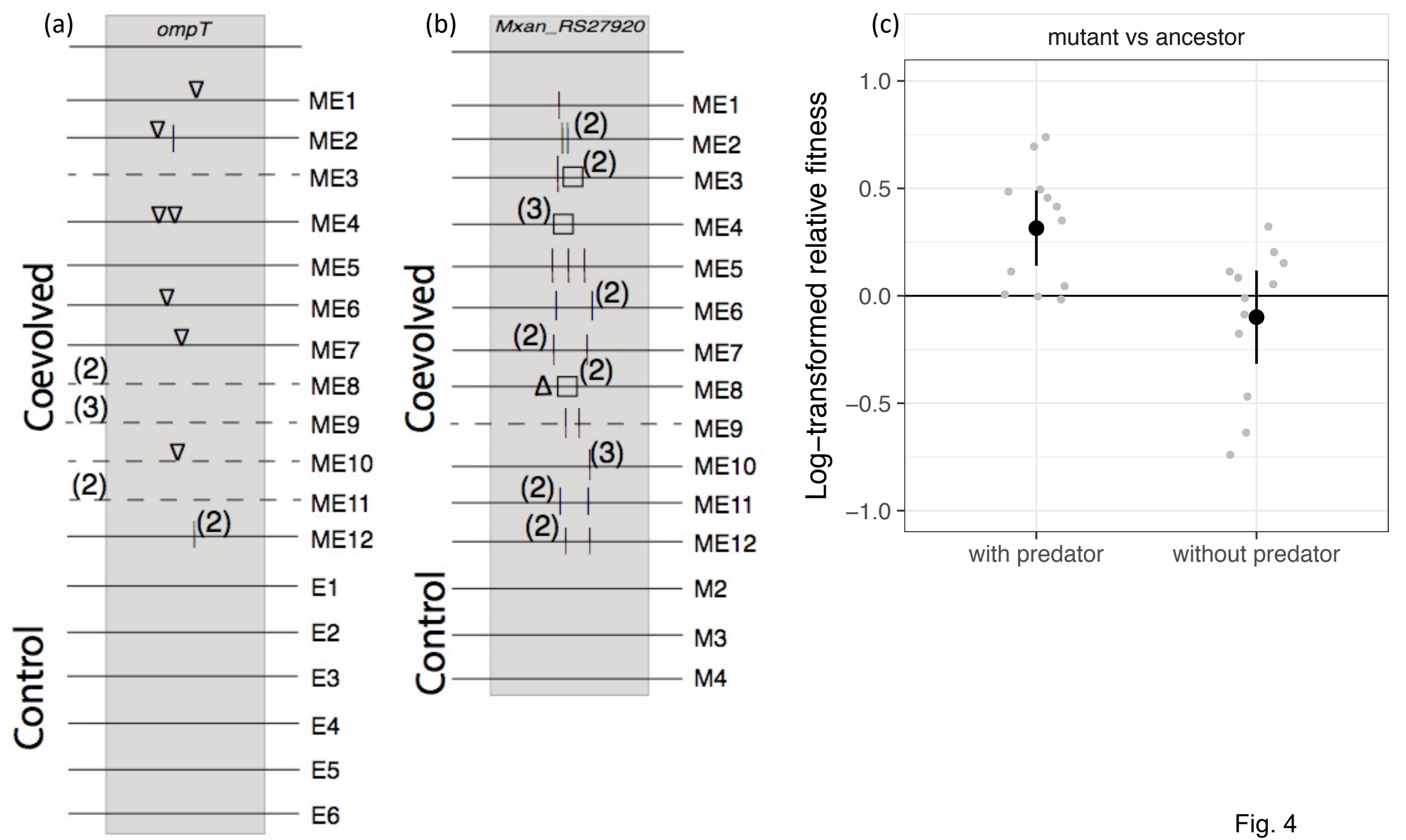
(a)
ompT
ME1
ME2
ME3
ME4
ME5
ME6
ME7
ME8
ME9
ME10
ME11
ME12
E1
E2
E3
E4
E5
E6
Coevolved
Control
(b)
Mxan_RS27920
ME1
ME2
ME3
ME4
ME5
ME6
ME7
ME8
ME9
ME10
ME11
ME12
M2
M3
M4
Coevolved
Control
(c)
mutant vs ancestor
Log−transformed relative fitness
1.0
0.5
0.0
−0.5
−1.0
with predator
without predator

Fig. 4

Extended data

Figure legends

Fig. S1: Prey adaptation to predation. Log-transformed relative fitness of each coevolved prey over control-evolved prey when grown in the presence and in the absence of predators. Each colour corresponds to one coevolved prey population.

Fig. S2: Predator adaptation to prey on glucose medium. Log-transformed relative fitness of each coevolved predator over ancestral predators when grown in the presence and in the absence of prey. Each colour corresponds to one coevolved predator population.

Fig. S3: Evolved prey relative fitness over ancestor. Log-transformed relative fitness of each coevolved and control-evolved prey population over ancestor in the presence of three different predator types.

Fig. S4: Schematic representation of Multiplex Freqseq. Adapted from Chubiz *et al* (2012). The bridging primer is made as in original reference. The first PCR reaction amplifies the genomic region that contains the mutation (yellow) identifying the two competitors. The reaction adds a M13f tail (blue) to the 5' end and a P7 tail (orange) to the 3' end that act as primer binding sites for the primers of next PCR reaction. The PCR products are purified using Ampure XP beads. The second PCR reaction adds the two barcodes (pink and dark blue) to the amplicon in a reaction involving three primers. The primer ABC1 (green) amplifies the bridging primer (blue) which in turn binds to the M13f priming site of the template DNA. The bridging primer along with the reverse primer (orange) adds the two barcodes to the amplicon. The samples are then pooled and purified to be used for Illumina sequencing.

Fig. S5: Validation of Multiplex Freqseq. Streptomycin resistant and sensitive strains of *E. coli* MG1655 were grown overnight, adjusted to an OD of 1 and mixed in different ratios before they were spun down and lysed to obtain DNA for frequency analysis by Multiplex Freqseq. The original tubes used to make the mixes were dilution plated to confirm they had equal densities. Grey ribbon around the line depicts 95% confidence intervals (n = 3 for each measurement).

Fig. S6: Fitness effect of ompT deletion. Log-transformed relative fitness of an *ompT*-deletion mutant in competition with the ancestor in the presence and in the absence of the ancestral predator (n = 6 for both treatments).

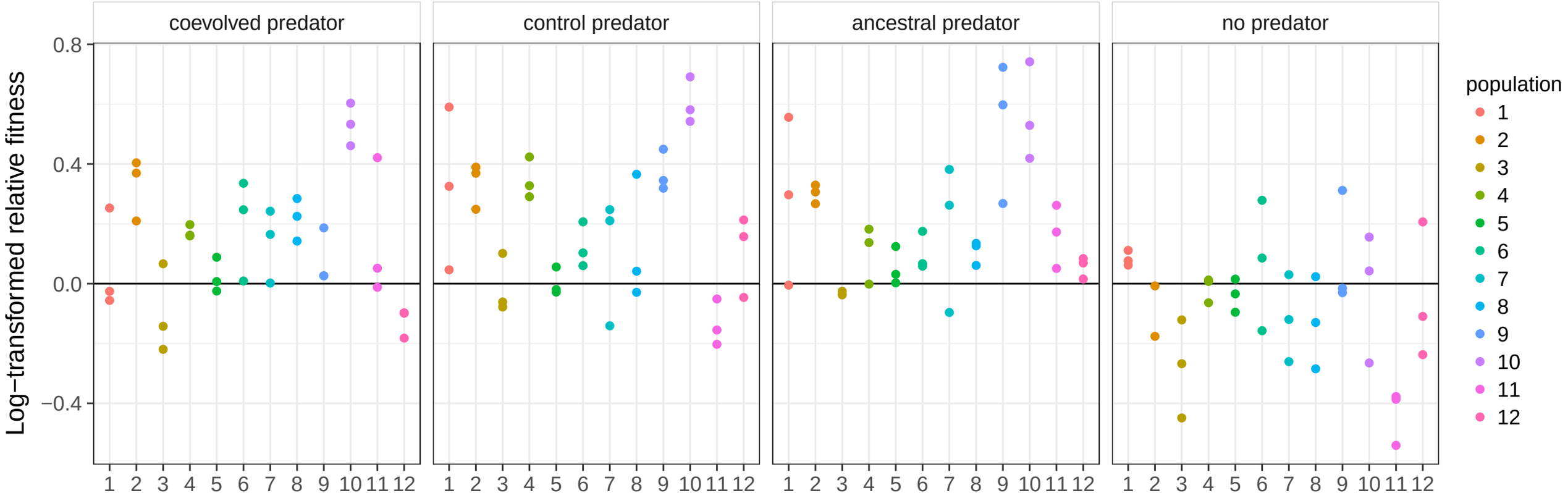
coevolved predator
control predator
ancestral predator
no predator
Log−transformed relative fitness
0.8
0.4
0.0
−0.4
1 2 3 4 5 6 7 8 9 10 11 12
population
1
2
3
4
5
6
7
8
9
10
11
12

Fig. S1

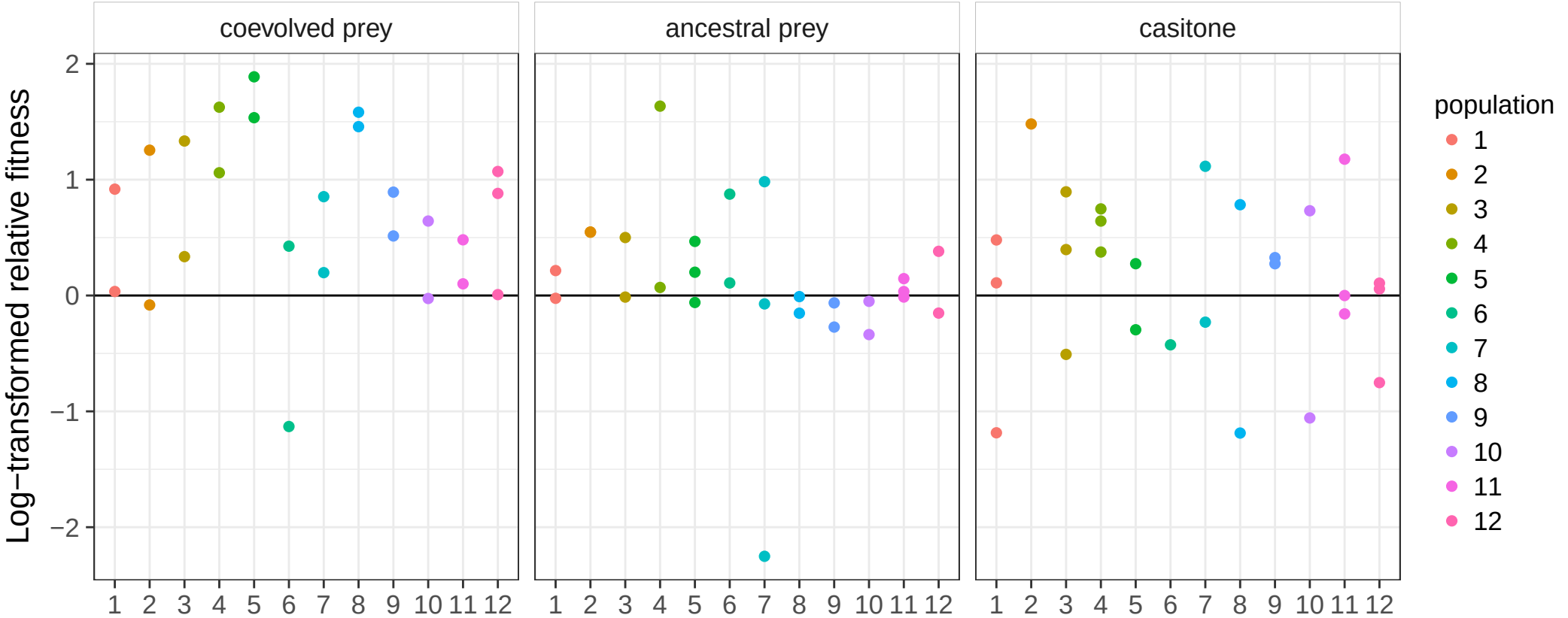
coevolved prey
ancestral prey
casitone
Log−transformed relative fitness
2
1
0
−1
−2
1 2 3 4 5 6 7 8 9 10 11 12
population
1
2
3
4
5
6
7
8
9
10
11
12

Fig. S2

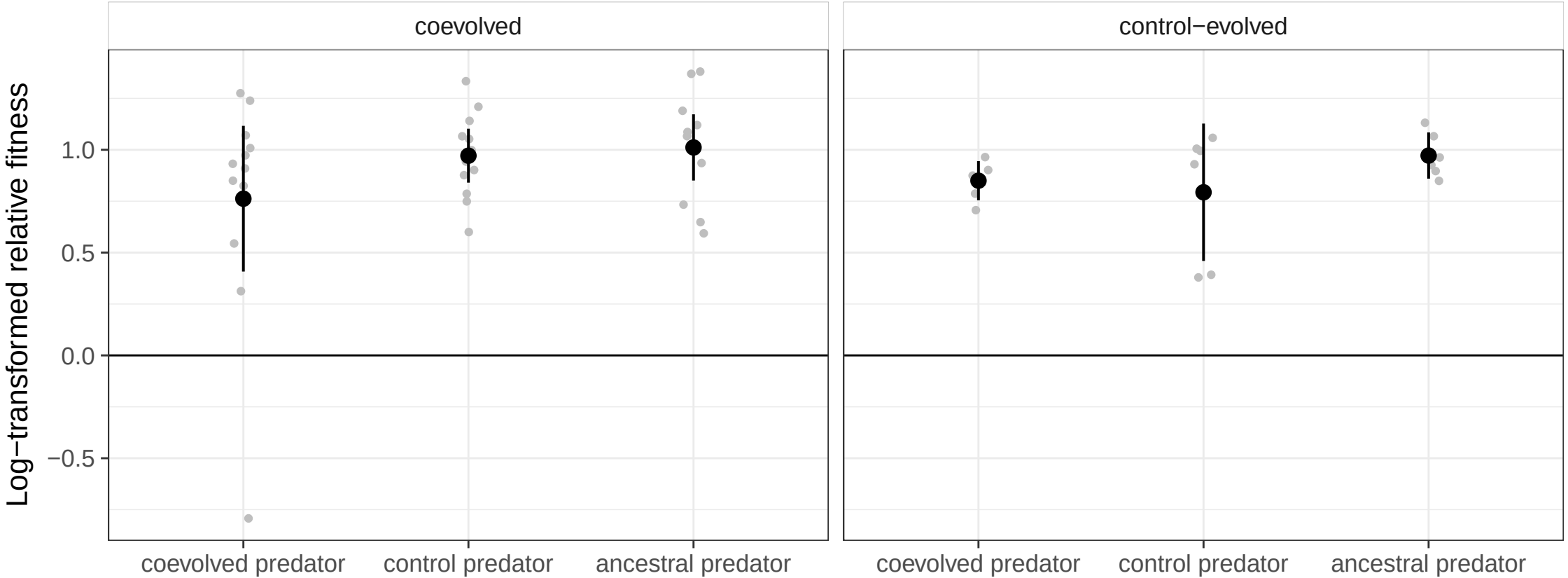
coevolved
control−evolved
Log−transformed relative fitness
1.0
0.5
0.0
−0.5
coevolved predator
control predator
ancestral predator
coevolved predator
control predator
ancestral predator

Fig. S3

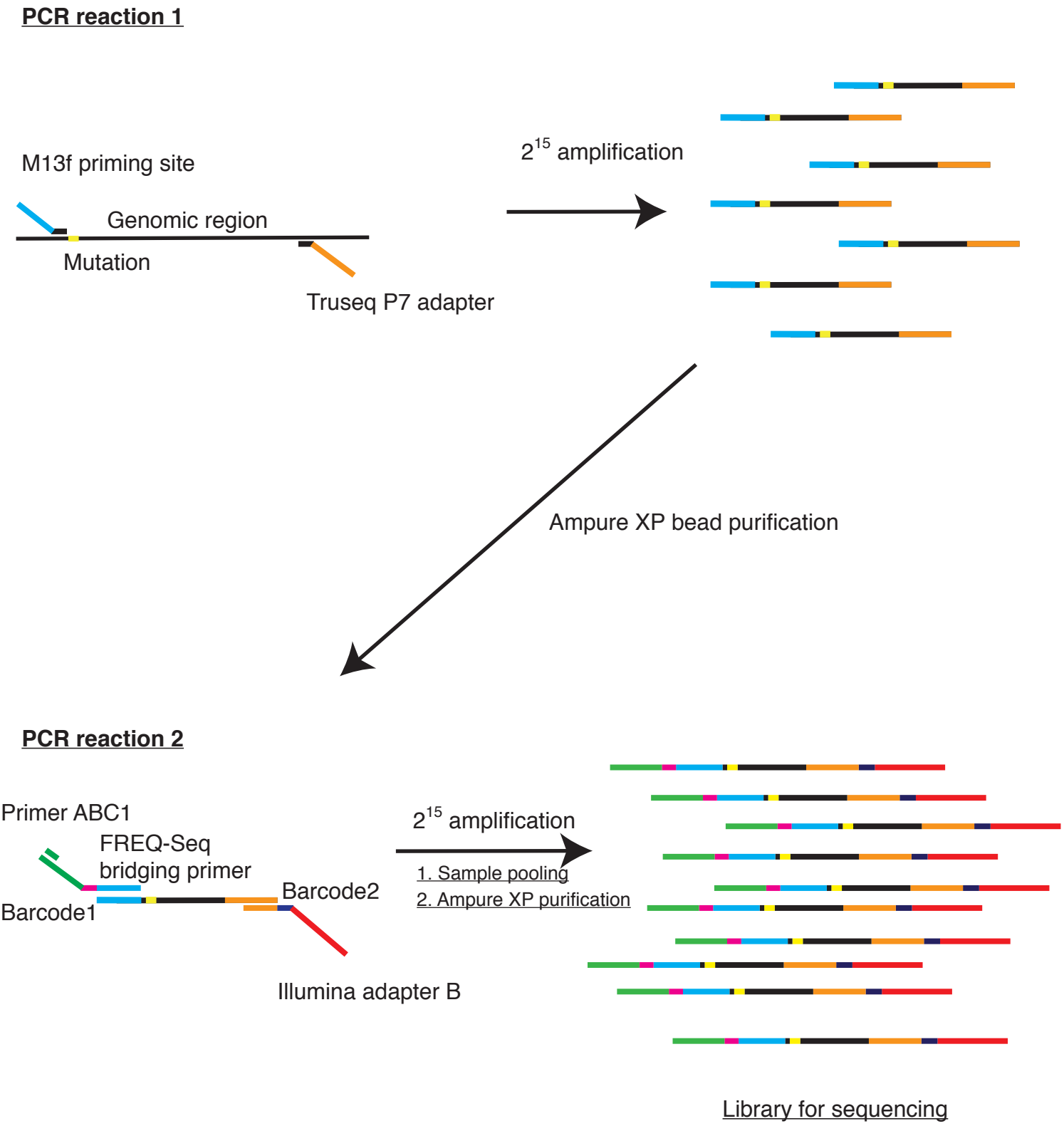

Fig. S4

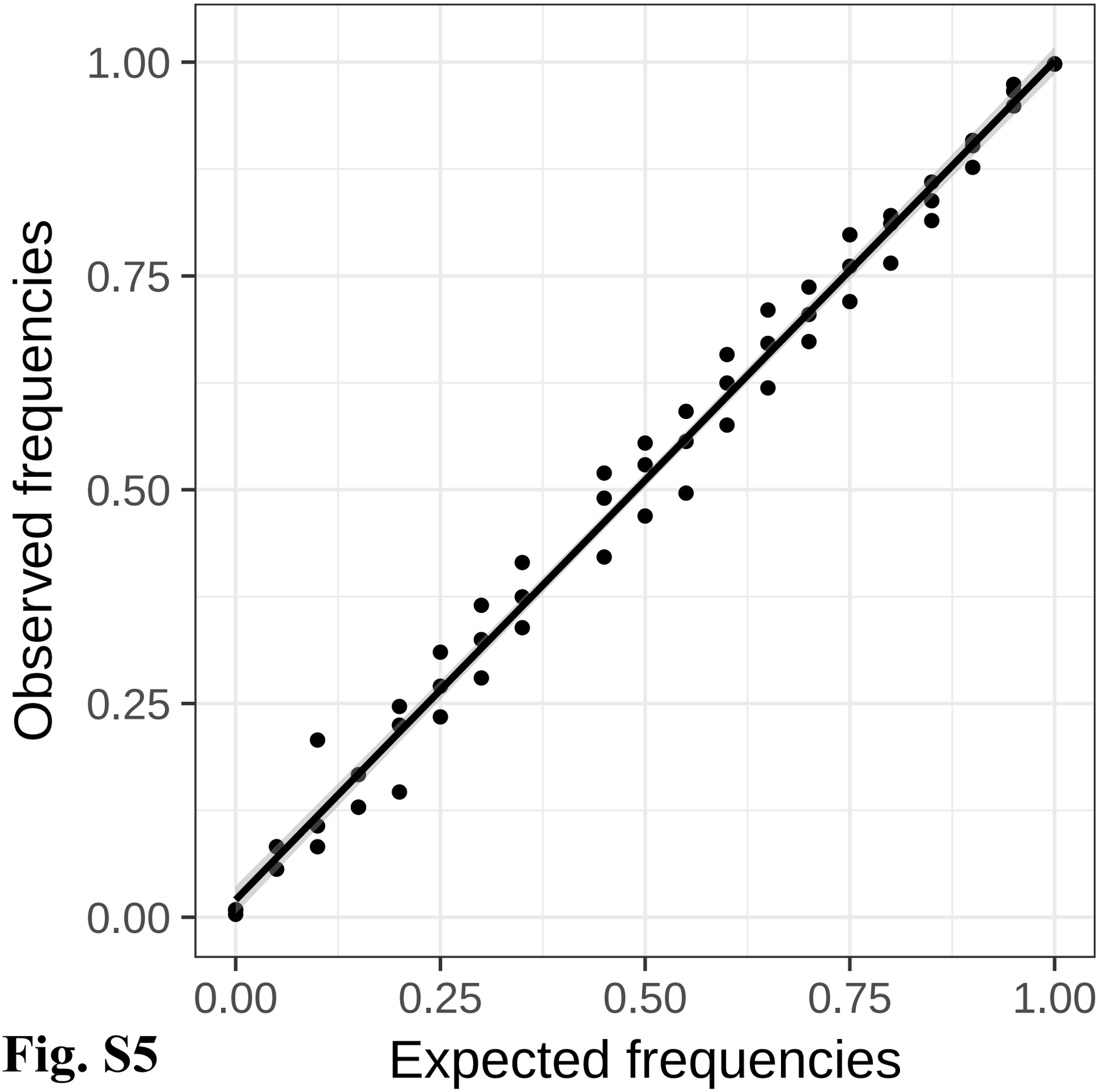
1.00
0.75
0.50
0.25
0.00
Observed frequencies
0.00
0.25
0.50
0.75
1.00
Expected frequencies

Fig. S5

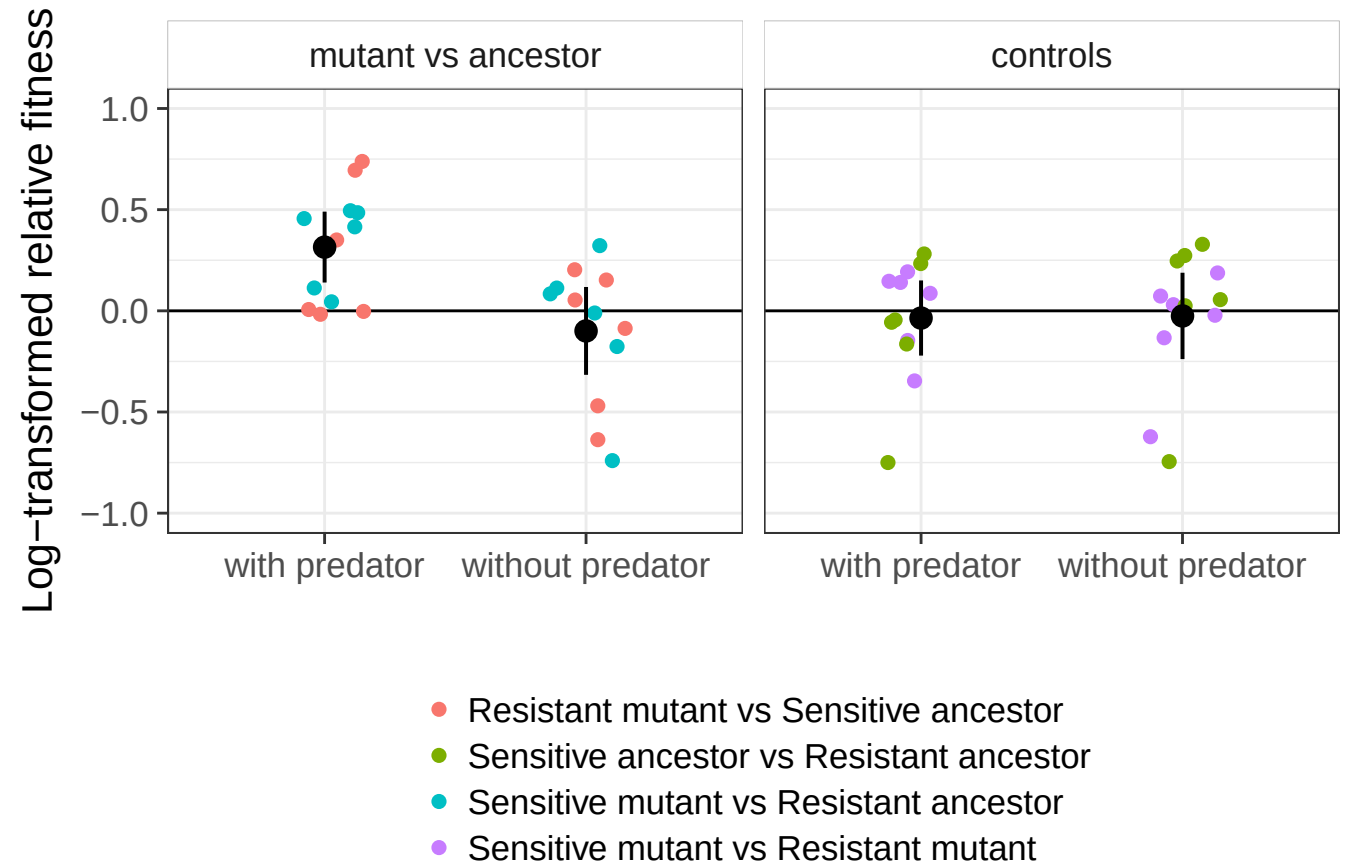
mutant vs ancestor
controls
Log−transformed relative fitness
1.0
0.5
0.0
−0.5
−1.0
with predator
without predator
with predator
without predator
Resistant mutant vs Sensitive ancestor
Sensitive ancestor vs Resistant ancestor
Sensitive mutant vs Resistant ancestor
Sensitive mutant vs Resistant mutant

Fig. S6

Table S1: Composition of the populations in the evolution experiment. Strep + (-) corresponds to streptomycin-resistant (sensitive) *E. coli* and Rif + (-) to rifampicin-resistant (sensitive) *M. xanthus*.

Population ID	Treatment	Composition	*E. coli*	*M. xanthus*
ME1	coevolved	ES1 – MS1	Strep -	Rif -
ME2	coevolved	ER1 – MR1	Strep +	Rif +
ME3	coevolved	ES2 – MS2	Strep -	Rif -
ME4	coevolved	ER2 – MR2	Strep +	Rif +
ME5	coevolved	ES3 – MS3	Strep -	Rif -
ME6	coevolved	ER3 – MR3	Strep +	Rif +
ME7	coevolved	ES1 – MR1	Strep -	Rif +
ME8	coevolved	ER1 – MS1	Strep +	Rif -
ME9	coevolved	ES2 – MR2	Strep -	Rif +
ME10	coevolved	ER2 – MS2	Strep +	Rif -
ME11	coevolved	ES3 – MR3	Strep -	Rif +
ME12	coevolved	ER3 – MS3	Strep +	Rif -
E1	control-evolved	ES1	Strep -	-
E2	control-evolved	ER1	Strep +	-
E3	control-evolved	ES2	Strep -	-
E4	control-evolved	ER2	Strep +	-
E5	control-evolved	ES3	Strep -	-
E6	control-evolved	ER3	Strep +	-
M1	control-evolved	MS1	-	Rif -
M2	control-evolved	MR1	-	Rif +
M3	control-evolved	MS2	-	Rif -
M4	control-evolved	MR2	-	Rif +
M5	control-evolved	MS3	-	Rif -
M6	control-evolved	MR3	-	Rif +

Table S2: Prey mutations. Accumulated mutations across three clones from each control-evolved (E1 to E6) and coevolved (ME1 to ME12) prey population. Multiple hits on the same gene in the same population correspond to different clones. Prey from ME1 is a hypermutator and is not included in this table.

Population	Position	Gene	Mutation	Annotation	In clone(s)
E01	1,979,391	*insA*/*uspC*	IS*1* +8 bp	intergenic (-176/-355)	1
	3,815,810	*pyrE*/*rph*	Δ1 bp	intergenic (-42/+24)	1
	4,182,820	*rpoB* →	C→T	H526Y (CAC→TAC)	2
E02	1,712,582	*nth*/*dtpA*	C→T	intergenic (+424/-187)	2
	3,815,810	*pyrE*/*rph*	Δ1 bp	intergenic (-42/+24)	2
	3,815,859	*rph* ←	Δ82 bp	pseudogene (610-691/716 nt)	1, 3
	4,608,449	*rimI* →	A→C	I89L (ATC→CTC)	3
E03	1,979,328	*insA*/*uspC*	IS*1* +9 bp	intergenic (-113/-417)	2
E04	3,938,971	*rbsR* →	A→T	M249L (ATG→TTG)	1
	3,815,883	*rph* ←	+C	pseudogene (667/716 nt)	1, 2, 3
	4,353,011	*ghoT* →	IS*5* +4 bp	coding (104-107/174 nt)	2, 3
E05	2,773,416	*yfjW* →	$(T)_{8\rightarrow7}$	coding (99/1704 nt)	2
E06	3,213,316	*rpoD* →	A→C	E90D (GAA→GAC)	2
	3,815,859	*rph* ←	Δ82 bp	pseudogene (610-691/716 nt)	1, 2, 3
ME2	584,808	*ompT* ←	IS*1* +8 bp	coding (819-826/954 nt)	3
	585,189	*ompT* ←	C→A	G149* (GGA→TGA)	2
	676,343	*ybeQ* ←	IS*5* +4 bp	coding (202-205/978 nt)	1
	1,879,829	*yeaR* ←	IS*186* +6 bp	coding (115-120/360 nt)	3
	3,815,859	*rph* ←	Δ82 bp	pseudogene (610-691/716 nt)	3
	3,815,921	*rph* ←	Δ1 bp	pseudogene (629/716 nt)	1, 2
	3,938,937	*rbsR* →	IS*2* +5 bp	coding (711-715/993 nt)	1
ME3	575,786	*[nmpC]–[ybdG]*	Δ27,775 bp	IS*5*-mediated	2

	3,231,367	*ygjK*/*fadH*	A→G	intergenic (+128/-298)	1
	3,378,982	*zapE* ←	A→G	L339P (CTG→CCG)	2
	3,815,806	*pyrE*/*rph*	A→C	intergenic (-38/+28)	2
	3,815,859	*rph* ←	Δ82 bp	pseudogene (610-691/716 nt)	1, 3
ME4	458,790	*clpX*/*lon*	IS*186* +6 bp	intergenic (+90/-93)	3
	585,015	*ompT* ←	IS*3* +4 bp	coding (616-619/954 nt)	1
	585,064	*ompT* ←	IS*3* +3 bp	coding (568-570/954 nt)	3
	1,188,482	*phoQ* ←	C→G	G432A (GGT→GCT)	3
	1,784,664	*fadK* →	IS*1* +9 bp	coding (1634-1642/1647 nt)	1
	3,815,859	*rph* ←	Δ82 bp	pseudogene (610-691/716 nt)	1, 2
	3,938,725	*rbsR* →	IS*5* +4 bp	coding (499-502/993 nt)	3
	4,237,542	*yjbG* →	T→G	Y216D (TAT→GAT)	3
	4,640,098	*arcA* ←	Δ1 bp	coding (209/717 nt)	3
ME5	1,405,766	*abgR*/*smrA*	G→A	intergenic (+117/-213)	1
	3,815,821	*pyrE*/*rph*	Δ13 bp	intergenic (-53/+1)	3
	3,815,859	*rph* ←	Δ82 bp	pseudogene (610-691/716 nt)	1, 2
ME6	585,171	*ompT* ←	IS*3* +3 bp	coding (461-463/954 nt)	1
	1,093,512	*ycdT* →	T→G	F213V (TTT→GTT)	3
	1,175,203	*ycfT*/*lolC*	A→T	intergenic (-38/-224)	3
	1,879,829	*yeaR* ←	IS*186* +6 bp	coding (115-120/360 nt)	3
	2,023,656	*fliR* →	IS*5* +4 bp	coding (764-767/786 nt)	2, 3
	3,815,821	*pyrE*/*rph*	Δ13 bp	intergenic (-53/+1)	1, 2, 3
	4,236,362	*yjbF* →	IS*1* +9 bp	coding (101-109/639 nt)	2
	4,400,484	*hfq* →	G→C	R66P (CGC→CCC)	3
ME7	585,273	*ompT* ←	IS*3* +3 bp	coding (359-361/954 nt)	1, 2

	1,979,337	*insA*/*uspC*	IS*5* +4 bp	intergenic (-122/-413)	3
	2,002,297	*fliC* ←	G→A	S437F (TCC→TTC)	3
	3,334,767	*ispB*/*sfsB*	$(A)_{5\rightarrow4}$	intergenic (+86/-142)	2
	3,815,890	*rph* ←	+C	pseudogene (660/716 nt)	1, 2, 3
ME8	575,786	*[nmpC]–[nfrA]*	Δ13,232 bp	IS*5*-mediated	2
	1,274,489	*ychO* →	C→A	R236S (CGC→AGC)	2
	2,023,826	*fliR*/*rcsA*	Δ1 bp	intergenic (+148/-142)	3
	3,461,564	*gspH* →	G→A	E33K (GAG→AAG)	1
	3,815,859	*rph* ←	Δ82 bp	pseudogene (610-691/716 nt)	1, 3
	3,848,559	*uhpC* ←	G→A	A22A (GCC→GCT)	2
	4,235,895	*pgi* → / → *yjbE*	IS*1* +9 bp	intergenic (+488/-3)	3
ME9	566,524	*[peaD]–[cusC]*	Δ30,005 bp	43 genes	1, 2, 3
	1,299,438	*ychE*/*oppA*	G→T	intergenic (+193/-1744)	1, 2, 3
	3,815,859	*rph* ←	Δ82 bp	pseudogene (610-691/716 nt)	1, 2, 3
	3,939,028	*rbsR* →	IS*2* +5 bp	coding (802-806/993 nt)	1, 2, 3
ME10	575,786	*[nmpC]–[nfrA]*	Δ14,013 bp	IS*5*-mediated	1
	585,064	*ompT* ←	IS*3* +3 bp	coding (568-570/954 nt)	3
	3,815,859	*rph* ←	Δ82 bp	pseudogene (610-691/716 nt)	1, 2
	3,853,838	*tisB*/*emrD*	C→T	intergenic (+196/-84)	2
	3,938,786	*rbsR* →	Δ20 bp	coding (560-579/993 nt)	3
	3,939,062	*rbsR* →	IS*2* +5 bp	coding (836-840/993 nt)	1, 2
ME11	458,790	*clpX*/*lon*	IS*186* +6 bp	intergenic (+90/-93)	3
	575,786	*[nmpC]–[ompT]*	Δ9,723 bp	IS*5*-mediated	1, 2
	732,995	*rhsC* →	C→T	T1138M (ACG→ATG)	3
	3,334,251	*ispB* →	G→A	C181Y (TGT→TAT)	3

	3,815,859	*rph* ←	Δ82 bp	pseudogene (610-691/716 nt)	1, 2, 3
	4,238,031	*yjbH* →	C→T	T133M (ACG→ATG)	3
	4,556,002	*yjiC* ←	IS*5* +4 bp	coding (316-319/831 nt)	3
ME12	458,790	*clpX*/*lon*	IS*186* +6 bp	intergenic (+90/-93)	3
	585,673	*ompT*/*pauD*	A→C	intergenic (-40/-384)	1, 2
	1,299,432	*ychE*/*oppA*	G→T	intergenic (+187/-1750)	3
	1,583,303	*ydeO* ←	IS*5* +4 bp	coding (382-385/762 nt)	1
	2,176,279	*gatZ* ←	IS*1* +9 bp	coding (35-43/1263 nt)	3
	2,565,938	*eutA* ←	C→T	G316D (GGC→GAC)	3
	3,815,810	*pyrE*/*rph*	Δ1 bp	intergenic (-42/+24)	1, 2
	3,938,996	*rbsR* →	T→A	L257* (TTA→TAA)	3
	4,238,888	*yjbH* →	IS*1* +8 bp	coding (1255-1262/2097 nt)	3
	4,640,418	*yjjY* →	IS*30* +2 bp	coding (17-18/141 nt)	3

Mutations and annotations follow standard breseq format. Flanking genes are mentioned for mutations in intergenic regions (e.g., *insA*/*uspC*). The nucleotide position corresponding to flanking genes is mentioned in brackets in the annotation column with + indicating position downstream of the stop codon and – indicating nucleotide upstream of the start codon of the following gene. SNPs are mentioned with an arrow and detail the corresponding amino-acid change for non-synonymous substitutions. Δ represents deletions, and for IS mediated mutations, corresponding IS element is mentioned as per reference-genome annotation. Large deletions mention first and last gene in the deleted segment in square brackets (e.g., *[nmpC]–[ybdG])*. * indicates change to stop codon.

Table S3: Genes mutated in prey. Mutations in genes or upstream of genes in *E. coli* from the evolution experiment. Numbers and brackets indicate in how many clones and populations, respectively, the gene was mutated. Mutations from *E. coli* from ME1 and synonymous SNPs are not included in the table. Mutations in rows 2-5 are big deletions for which the first and last gene are mentioned (all four deletions encompass *ompT*).

Gene(s) or upstream of gene	Control (#)	Coevolved (#)	Total (#)
clpX	0	3(3)	3(3)
[peaD]–[cusC]	0	3(1)	3(1)
[nmpC]–[ompT]	0	2(1)	2(1)
[nmpC]–[nfrA]	0	2(2)	2(2)
[nmpC]–[ybdG]	0	1	1
ompT	0	11(6)	11(6)
ybeQ	0	1	1
rhsC	0	1	1
ycdT	0	1	1
ycfT	0	1	1
phoQ	0	1	1
ychO	0	1	1
oppA	0	4(2)	4(2)
smrA	0	1	1
ydeO	0	1	1
dtpA	1	0	1
fadK	0	1	2
yeaR	0	2(2)	2(2)
insA / *uspC**	2(2)	1	3(3)
fliC	0	1	1
fliR	0	2(2)	2(2)
rcsA	0	1	1
gatZ	0	1	1
eutA	0	1	1
yfjW	1	0	1
rpoD	1	0	1
fadH	0	1	1
ispB	0	1	1
sfsB	0	1	1
zapE	0	1	1
gspH	0	1	1
rph	10(4)	29(11)	39(15)

emrD	0	1	1
rbsR	1	10(6)	11(7)
rpoB	1	0	1
*yjbEFGH***	0	5(4)	5(4)
ghoT	2(1)	0	2(1)
hfq	0	1	1
yjiC	0	1	1
rimI	1	0	1
arcA	0	1	1
yjjY	0	1	1

*Genes face each other and mutation is seen in the intergenic region, thus upstream of both genes

**Functional operon involved in polysaccharide transport

Table S4: Predator mutations. Accumulated mutations across three clones from each control-evolved (M2 to M4) and coevolved (ME1 to ME12) predator population. Multiple hits on the same gene in the same population correspond to different clones. All three predator clones from ME4 and two clones from ME8 are hypermutators and are not included in this table.

Pop.	Position	Gene	Mutation	Annotation	In clone(s)
M2	335,653	*MXAN_RS01385*	C→A	Y55* (TAC→TAA)	2
	1,837,263	*MXAN_RS07605*	G→T	L31F (TTG→TTT)	3
	3,600,700	*MXAN_RS14915*	A→T	H548L (CAC→CTC)	2,3
	6,885,348	*MXAN_RS26830/ MXAN_RS26835*	A→G	intergenic (+1934/+1898)	3
	7,536,463	*MXAN_RS29545*	T→G	S142R (AGC→CGC)	3
M3	2,634,706	*MXAN_RS10970*	C→T	G630D (GGC→GAC)	1,2,3
	7,266,486	*MXAN_RS28390*	T→G	Y262D (TAC→GAC)	1,2,3
M4	1,837,910	*MXAN_RS07605*	G→T	S247I (AGC→ATC)	2
	2,104,526	*MXAN_RS08605*	C→T	P39S (CCC→TCC)	1
	3,600,700	*MXAN_RS14915*	A→T	H548L (CAC→CTC)	1,2,3
	5,275,860	*MXAN_RS20850*	G→T	A980E (GCG→GAG)	1
	7,266,516	*MXAN_RS28390*	G→T	G272C (GGC→TGC)	1
ME1	846,285	*MXAN_RS03570*	A→G	R12R (CGA→CGG)	1
	3,110,383	*MXAN_RS12885*	G→A	G449R (GGG→AGG)	1
	7,128,080	*MXAN_RS27920*	G→C	G59A (GGC→GCC)	1
ME2	3,600,700	*MXAN_RS14915*	A→T	H548L (CAC→CTC)	1,2,3
	4,835,633	*MXAN_RS19305*	C→T	A154T (GCG→ACG)	1,2
	5,245,952	*MXAN_RS20780*	G→C	G431G (GGC→GGG)	1
	6,783,715	*MXAN_RS26430*	A→C	D483A (GAC→GCC)	1
	7,128,607	*MXAN_RS27920*	A→C	T235P (ACG→CCG)	3
	7,128,784	*MXAN_RS27920*	G→T	E294* (GAG→TAG)	1,2
	7,405,346	*MXAN_RS29015*	C→T	Q56* (CAG→TAG)	1
ME3	1,099,133	*MXAN_RS04600*	C→A	T325T (ACC→ACA)	1,2,3
	3,103,710	*MXAN_RS12865 / MXAN_RS12870*	C→T	intergenic (-17/+70)	1,2,3
	7,128,379	*MXAN_RS27920*	G→A	A159T (GCG→ACG)	2
	7,128,860	*MXAN_RS27920*	(CTGAA) 1→2	coding (956/1269 nt)	1,3
ME5	3,013,847	*MXAN_RS12525*	G→T	A98E (GCG→GAG)	1
	3,107,516	*MXAN_RS12875*	A→C	L207R (CTC→CGC)	3

	3,111,550	*MXAN_RS12890*	G→T	R325L (CGC→CTC)	1
	3,600,700	*MXAN_RS14915*	A→T	H548L (CAC→CTC)	2
	4,990,717	*MXAN_RS19805*	C→T	L138L (CTG→CTA)	2
	6,868,901	*MXAN_RS26750*	C→A	A92E (GCG→GAG)	1,3
	7,127,967	*MXAN_RS27920*	T→A	Y21* (TAT→TAA)	2
	7,128,926	*MXAN_RS27920*	C→G	P341R (CCC→CGC)	3
	7,128,928	*MXAN_RS27920*	A→T	I342F (ATC→TTC)	3
	7,128,968	*MXAN_RS27920*	G→T	R355L (CGA→CTA)	1
ME6	3,600,700	*MXAN_RS14915*	A→T	H548L (CAC→CTC)	1,2,3
	7,128,205	*MXAN_RS27920*	G→C	G101R (GGG→CGG)	2
	7,128,992	*MXAN_RS27920*	T→A	V363E (GTG→GAG)	1,3
ME7	190,820	*MXAN_RS00760 / MXAN_RS00765*	(C)7→6	intergenic (-221/-160)	2
	447,814	*MXAN_RS01880*	T→C	F197S (TTC→TCC)	2
	1,923,559	*MXAN_RS07875*	G→T	T792T (ACG→ACT)	1
	3,013,847	*MXAN_RS12525*	G→T	A98E (GCG→GAG)	1,3
	3,600,700	*MXAN_RS14915*	A→T	H548L (CAC→CTC)	1,2,3
	4,779,681	*MXAN_RS19125*	T→G	S1372R (AGC→CGC)	2
	7,128,142	*MXAN_RS27920*	G→A	G80R (GGG→AGG)	1,3
	7,128,944	*MXAN_RS27920*	T→A	V347D (GTC→GAC)	2
	8,557,472	*MXAN_RS33865*	C→T	L700L (CTG→CTA)	2
ME8	1,202,985	*MXAN_RS04945*	+TTC	coding (666/1143 nt)	3
	7,127,965	*MXAN_RS27920*	Δ1 bp	coding (61/1269 nt)	3
	8,560,499	*MXAN_RS33870 / MXAN_RS33875*	T→C	intergenic(-91/-340)	3
ME9	3,107,516	*MXAN_RS12875*	A→C	L207R(CTC→CGC)	3
	4,780,726	*MXAN_RS19125*	(C)8→7	coding(3069/26949nt)	1
	6,868,901	*MXAN_RS26750*	C→A	A92E(GCG→GAG)	3
	7,125,516	*[MXAN_RS27905]-[MXAN_RS27930]*	Δ5,485bp		2
	7,128,926	*MXAN_RS27920*	C→G	P341R(CCC→CGC)	3
	7,128,928	*MXAN_RS27920*	A→T	I342F(ATC→TTC)	3
	7,129,049	*MXAN_RS27920*	C→T	A382V(GCG→GTG)	1
	7,133,777	*MXAN_RS27935*	T→G	S120R(AGC→CGC)	2
	8,065,362	*MXAN_RS31715*	G→T	E669*(GAA→TAA)	2
ME10	865,277	*MXAN_RS03650*	C→T	T270T(ACG→ACA)	1
	1,099,133	*MXAN_RS04600*	C→A	T325T(ACC→ACA)	1,2,3

	3,103,710	*MXAN_RS12865 / MXAN_RS12870*	C→T	intergenic(-17/+70)	1,2,3
	7,129,100	*MXAN_RS27920*	T→G	L399R(CTC→CGC)	1,2,3
ME11	1,295,240	*MXAN_RS05350*	G→A	L33L(CTG→TTG)	3
	3,013,847	*MXAN_RS12525*	G→T	A98E(GCG→GAG)	3
	3,600,700	*MXAN_RS14915*	A→T	H548L(CAC→CTC)	1,2,3
	3,757,170	*MXAN_RS15525*	G→C	N62K(AAC→AAG)	1,3
	7,128,515	*MXAN_RS27920*	A→C	D204A(GAT→GCT)	1,3
	7,129,015	*MXAN_RS27920*	G→A	D371N(GAC→AAC)	2
ME12	1,055,109	*MXAN_RS04445*	A→C	D244A(GAC→GCC)	3
	3,013,847	*MXAN_RS12525*	G→T	A98E(GCG→GAG)	3
	3,108,002	*MXAN_RS12875*	G→A	S45L(TCG→TTG)	2
	6,696,636	*MXAN_RS26090 / MXAN_RS26095*	T→C	intergenic(-172/-68)	1
	6,868,901	*MXAN_RS26750*	C→A	A92E(GCG→GAG)	1,2,3
	6,925,823	*MXAN_RS27010*	G→A	P119L(CCG→CTG)	2
	6,958,933	*MXAN_RS27125*	C→T	A557T(GCG→ACG)	1
	7,128,926	*MXAN_RS27920*	C→G	P341R(CCC→CGC)	1,2
	7,128,928	*MXAN_RS27920*	A→T	I342F(ATC→TTC)	1,2
	7,129,072	*MXAN_RS27920*	G→A	A390T(GCC→ACC)	3

Table S5: Genes mutated in predator. Mutations in genes or upstream of genes in *M. xanthus* from the evolution experiment. Numbers and brackets indicate in how many clones and populations, respectively, the gene was mutated. Mutations from all three ME4 predator clones, two ME8 clones and synonymous SNPs are not included in the table.

Gene(s) or upstream of gene	Control (#)	Coevolved (#)	Total (#)
MXAN_RS00760 / MXAN_RS00765	0	1(1)	1(1)
MXAN_RS01385	1(1)	0	1(1)
MXAN_RS01880	0	1(1)	1(1)
MXAN_RS03570	0	1(1)	1(1)
MXAN_RS03650	0	1(1)	1(1)
MXAN_RS04445	0	1(1)	1(1)
MXAN_RS04600	0	6(2)	6(2)
MXAN_RS05350	0	1(1)	1(1)
MXAN_RS07605	2(2)	0	2(2)
MXAN_RS07875	0	1(1)	1(1)
MXAN_RS08605	1(1)	0	1(1)
MXAN_RS10970	3(1)	0	3(1)
MXAN_RS12525	0	5(4)	5(4)
MXAN_RS12865	0	6(2)	6(2)
MXAN_RS12875	0	4(4)	4(4)
MXAN_RS12885	0	1(1)	1(1)
MXAN_RS12890	0	1(1)	1(1)
MXAN_RS14915	8(3)	15(6)	23(9)
MXAN_RS15525	0	2(1)	2(1)
MXAN_RS17875	0	1(1)	1(1)
MXAN_RS19125	0	2(2)	2(2)
MXAN_RS19305	0	2(1)	2(1)
MXAN_RS19805	0	1(1)	1(1)
MXAN_RS20780	0	1(1)	1(1)
MXAN_RS20850	1(1)	0	1(1)
MXAN_RS26090 / MXAN_RS26095	0	1(1)	1(1)
MXAN_RS26430	0	1(1)	1(1)
MXAN_RS26750	0	6(3)	6(3)
MXAN_RS26830 / MXAN_RS26835	1(1)	0	1(1)
MXAN_RS27010	0	1(1)	1(1)
MXAN_RS27125	0	1(1)	1(1)
[MXAN_RS27905]–[MXAN_RS27930]	0	1(1)	1(1)
MXAN_RS27920	0	28(12)	28(12)
MXAN_RS27935	0	1(1)	1(1)
MXAN_RS28390	4(2)	0	4(2)
MXAN_RS29015	0	1(1)	1(1)
MXAN_RS29545	1(1)	0	1(1)
MXAN_RS31715	0	1(1)	1(1)

MXAN_RS33865	0	1(1)	1(1)

Table S6: List of primers used for Multiplex FreqSeq. Right-side and left-sided barcodes are emboldened.

*NNNNNN denotes the 6-nt barcode and is the same as those used by Chubiz *et al* (2012).

Name		**Sequence** (5'- 3')
For bridging primer synthesis		
Forward primer ABC1		AATGATACGGCGACCAC
Reverse primer ABC2		ACTGGCCGTCGTTTTAC
For FreqSeq PCR reaction 1		
Forward primer for *E. coli* (M13f tail) + genomic region		(GTAAAACGACGGCCAGT) GCAAAAACGTGGCGTATGTA
Reverse primer for *E. coli* (P7) + genomic region		(GATCGGAAGAGCACACGTCTGAACTCCAGTCA) TGACCTTCACCACCGATGTA
Forward primer for *M. xanthus* (M13f tail) + genomic region		(GTAAAACGACGGCCAGT) AGACGAACCCCCTGTCCGAA
Reverse primer for *M. xanthus* (reverse complement of P7) + genomic region		(TGACTGGAGTTCAGACGTGTGCTCTTCCGATC) ATGGGGCAGATGCGGCCGTA
For FreqSeq PCR reaction 2		
Forward primer ABC1		AATGATACGGCGACCAC
Bridging primer*		(AATGATACGGCGACCACCGAGATCTACACTCTTTCCCTACAC GACGCTCTTCCGATCT) (**NNNNNN**) (GTAAAACGACGGCCAGT)
Reverse primer with left-sided barcode (Illumina-B adapter) + (**barcode**) + (P7) for *E. coli*	BCe_01	(CAAGCAGAAGACGGCATACGAGAT) (**AGCAAT**) (GATCGGAAGAGCACACG)
	BCe_02	(CAAGCAGAAGACGGCATACGAGAT) (**CCTGTT**) (GATCGGAAGAGCACACG)
	BCe_03	(CAAGCAGAAGACGGCATACGAGAT) (**GGGTTT**) (GATCGGAAGAGCACACG)
	BCe_04	(CAAGCAGAAGACGGCATACGAGAT) (**GAAGGC**) (GATCGGAAGAGCACACG)
	BCe_46	(CAAGCAGAAGACGGCATACGAGAT) (**GGATTA**) (GATCGGAAGAGCACACG)
	BCe_47	(CAAGCAGAAGACGGCATACGAGAT) (**TATATA**) (GATCGGAAGAGCACACG)
	BCe_48	(CAAGCAGAAGACGGCATACGAGAT) (**GTACAA**) (GATCGGAAGAGCACACG)
Reverse primer with left-sided barcode (Illumina-B adapter) + (**barcode**) + (P7) for *M. xanthus*	BCm_01	(CAAGCAGAAGACGGCATACGAGAT) (**AGCAAT**) (TGACTGGAGTTCAGACG)
	BCm_02	(CAAGCAGAAGACGGCATACGAGAT) (**CCTGTT**) (TGACTGGAGTTCAGACG)
	BCm_03	(CAAGCAGAAGACGGCATACGAGAT) (**GGGTTT**) (TGACTGGAGTTCAGACG)
	BCm_46	(CAAGCAGAAGACGGCATACGAGAT) (**GGATTA**) (TGACTGGAGTTCAGACG)
	BCm_47	(CAAGCAGAAGACGGCATACGAGAT) (**TATATA**) (TGACTGGAGTTCAGACG)
	BCm_48	9CAAGCAGAAGACGGCATACGAGAT) (**GTACAA**) (TGACTGGAGTTCAGACG)

Table S7: PCR conditions for Multiplex FreqSeq

FreqSeq	DNA template	PCR mix	Cycling conditions
PCR1	Lysate of whole populations	2.5 µL Forward primer 2.5 µL Reverse primer 25 µL Phusion master mix 1.5 µL DMSO 8.0 µL DNA 10.5 µL water (to make a final volume of 50 µl)	98 °C – 2 mins Cycle 15x: 98 °C – 10 s 56 °C (prey) or 57 °C (predator) – 30 s 72 °C – 30 s 72 °C – 7 mins 4 °C – <3 hrs or freeze
PCR2	Ampure XP bead purified product from PCR1	2.5 µL Forward primer ABC1 2.5 µL Reverse primer with left-sided barcode 25 µL Phusion master mix 1.5 µL DMSO 18.5 µL DNA 0.25 µM Bridging primer (volume to be determined according the DNA concentration of each primer)	98 °C – 3 mins Cycle 15x: 98 °C – 20 s 53 °C – 20 s 72 °C – 30 s 72 °C – 7 mins 4 °C – <3 hrs or freeze

Bash script used for Multiplex Freqseq

```
#Trims the Illumina adapter from the 3' end exposing the 6-nt barcode. Create adapter.fa file beforehand with the adapter sequence.
java -jar ~/trimmomatic-0.33.jar SE 1_S1_L001_R1_001.fastq.gz trimmed.fastq.gz ILLUMINACLIP:adapter.fa:2:30:10

#unzips the fastq file to be used by FASTX toolkit
gunzip trimmed.fastq.gz

#Create barcodes.txt file beforehand with all the right-side barcodes used
cat trimmed.fastq | fastx_barcode_splitter.pl --bcfile barcodes.txt --eol --mismatches 1 --prefix

#Demultiplexes the sequences as per the right-side barcodes
~/bla_ --suffix ".fastq"


#####Start here if demultiplexing has been done by the MiSeq machine#########

#invokes Freq-Out to determine ratio of each allele for each barcode
mono freqout.exe -xml=settings_rpsL.xml bla_BC1.fastq

#copies and renames the output from Freq-Out so that subsequent commands do not overwrite the previous output file
cp AF_Seq_Results.csv BC_01.csv

#repeat for each right-side barcode
mono freqout.exe -xml=settings_rpsL.xml bla_BC2.fastq
cp AF_Seq_Results.csv BC_02.csv
mono freqout.exe -xml=settings_rpsL.xml bla_BC3.fastq
cp AF_Seq_Results.csv BC_03.csv
mono freqout.exe -xml=settings_rpsL.xml bla_BC4.fastq
cp AF_Seq_Results.csv BC_04.csv
mono freqout.exe -xml=settings_rpsL.xml bla_BC46.fastq
cp AF_Seq_Results.csv BC_46.csv
mono freqout.exe -xml=settings_rpsL.xml bla_BC47.fastq
cp AF_Seq_Results.csv BC_47.csv
mono freqout.exe -xml=settings_rpsL.xml bla_BC48.fastq
cp AF_Seq_Results.csv BC_48.csv

#removes the original copy of last generated output file
rm AF_Seq_Results.csv
```